NGR 41189
NASACR-106378

AED R-3497
Issued: October 10, 1969

First Quarterly Report
Study to Determine and Improve Design for Lithium-Doped Solar Cells

Prepared for
Jet Propulsion Laboratory
California Institute of Technology
Pasadena, California
In fulfillment of
Contract No. 952555
June 24 to September 30, 1969

RCA

RCA Corporation | Defense Electronic Products
Astro Electronics Division | Princeton, New Jersey

AED R-3497
Issued: October 10, 1969

First Quarterly Report
Study to Determine and Improve Design for Lithium-Doped Solar Cells

Prepared for
Jet Propulsion Laboratory
California Institute of Technology
Pasadena, California
In fulfillment of
Contract No. 952555
June 24 to September 30, 1969

RCA Corporation | Defense Electronic Products
Astro Electronics Division | Princeton, New Jersey

PREFACE

This is the First Quarterly Report on a program for a "Study to Determine and Improve Design for Lithium-Doped Solar Cells." This report was prepared under Contract No. 952555 for Jet Propulsion Laboratory, Pasadena, California, by the Astro-Electronics Division of RCA, Princeton, New Jersey. The preparation of this report is a contractual requirement covering the period from June 24 to September 30, 1969. The work reported here was conducted by the Radiation Effects group, Manager, Dr. A.G. Holmes-Siedle. This group is a part of the Technology Development group of the Astro-Electronics Division, Manager, Mr. Martin Wolf, which is located at the RCA Space Center. The Project Supervisor is Dr. A.G. Holmes-Siedle and the Project Scientist is Dr. G.J. Brucker. The Technical Monitor of the program is Mr. Paul Berman of the Solar Power group, Jet Propulsion Laboratory.

ABSTRACT

This is the First Quarterly Report on a program to study and analyze the action of lithium in producing a recovery of radiation damage in bulk silicon and silicon solar cells. This program has technical continuity with the work performed by RCA-AED for JPL on Contract No. 952249. The eventual goal of this effort is to understand the damage and recovery mechanisms so that an optimum set of design rules can be specified.

The test vehicles used for this work are (1) a group of solar cells supplied by JPL, and (2) silicon bars in the "Hall-bar" configuration. The source of particle irradiation being used is a 1-MeV electron beam produced by the RCA Laboratories Van de Graaff generator.

Technical progress during this reporting period includes preliminary Hall and resistivity measurements which indicate that as the lithium concentration in the Hall samples decreases, the curve of carrier-removal rate vs temperature appears to shift along the temperature axis to lower temperatures while carrier removal at higher bombardment temperatures (T_B = 140° K - 297° K) appears to decrease. Recovery time constants of Hall samples allowed to anneal at room temperature were longer at lower lithium concentrations, this being in agreement with previous results obtained for minority-carrier properties in solar cells. Further evidence was obtained for the dissociation of the LiV defect and the formation of complexes between lithium and acceptor defects during the annealing of irradiated Hall samples at 297° K.

Measurements of minority-carrier diffusion length versus temperature on two lithium solar cells made from antimony-doped, oxygen-rich silicon and irradiated to 3×10^{15} e/cm^2 at 77°K, indicate the generation of a defect at an energy level of approximately E_C - 0.16 eV (probably an A-center). During a six-hour, 373°K anneal, both cells displayed significant lifetime recovery with approximately first-order kinetics, the kinetics observed previously in annealing of solar cells containing lithium. An unusual feature, however, was that the cell more heavily doped with antimony showed a much slower recovery rate than the more lightly doped cell.

Stability tests were continued on cells from JPL shipments No. 1 to 3 and were initiated on cells from shipments No. 4 and 5. Only small ($\approx$ 3%) room-temperature recovery from oxygen-rich silicon was observed in antimony-doped (Lot C2) cells made 280 days after irradiation to 1×10^{14} e/cm^2. This is much less than anticipated in view of the concentrations of lithium thought to have been introduced into the cell and confirms the above-mentioned evidence of a special participation of the background donor, antimony, in the damage recovery process.

TABLE OF CONTENTS

LIST OF ILLUSTRATIONS

LIST OF TABLES

SECTION I
INTRODUCTION

A. GENERAL

This contract effort represents an experimental investigation of the physical properties of lithium-containing p-on-n solar cells and bulk silicon samples, and of the processes which occur in these devices and samples before and after irradiation. The program objectives are to develop and reduce-to-practice analytical techniques to characterize the radiation resistance of lithium-doped solar cells and its dependence on the materials and processes used to fabricate them. On the basis of this and other data, RCA-AED will determine and recommend an improved design of lithium-doped solar cells for space use. A previous RCA program (Ref. 1) performed for JPL provided the groundwork for this effort.

B. TECHNICAL APPROACH

The approach to the objectives is based on the irradiation and measurement of the electrical properties of bulk-silicon samples, government-furnished (GFE) solar cells, and in-house fabricated test-diodes (Ref. 1). Experiments on bulk samples are to include Hall and resistivity measurements taken as a function of (1) bombardment temperature, (2) resistivity, (3) fluence, (4) oxygen concentration, and (5) annealing time at toom temperature. Diffusion length measurements on solar cells and test diodes are to be made as a function of the same five parameters as for bulk samples. In addition, capacitance and I-V measurements are to be made on selected cells. Stability studies are to be conducted on solar cells, which will be irradiated and observed for long periods of time. Based on these results, a set of preliminary design rules and specifications will be determined, and solar cells will be procured by JPL in accordance with these rules. As a check of the validity of the design rules, tests will be conducted on this group of cells and a set of modified design rules will be derived.

C. SUMMARY OF PREVIOUS WORK

A brief history is given here of the recent work performed on a preceding contract (Ref. 1) for purposes of continuity and to provide the reader with a better understanding of the current technical approach, its problems, and objectives.

In the work of the past year, basic material studies and device studies were pursued in parallel. These studies produced significant advances in the understanding of the defect interactions, dynamics, and general properties of lithium solar

cells. The dynamics of lithium in silicon have been studied under conditions analogous to those which would be experienced in a practical lithium solar-cell array over several years in a high-fluence trapped space-radiation situation, such as might be encountered near Earth, Jupiter, or other planets.

As a result of this, and the work of other contractors funded by JPL in the 1967-1969 period, the general level of confidence and knowledge as to what is happening in lithium cells has increased in many ways.

In the RCA work, tests on GFE cells irradiated to fluences from 10^{14} to 10^{16} e/cm^2 indicated that, to obtain good long-term stability in cells made from silicon of low oxygen content, the lithium density should be made as low as is compatible with maximum cell recovery for the fluence applied to the cells. Cells with high lithium concentration and steep gradients of lithium density near the junction showed gross lithium motion near the junction over approximately one year. Cells of this type have redegraded as much as 35 percent eleven months after bombardment to 10^{14} e/cm^2.

The RCA investigators found that redegradation in power output was due to curve-shape changes and decreases in open-circuit voltage as well as changes in short-circuit current. Cells with smaller lithium-density gradient showed better stability both before bombardment and after bombardment to 10^{14} e/cm^2.

Preliminary measurements made by the RCA investigators on solar cells made from float-zone refined silicon (FZ cells) indicated that the lithium-diffusion constant in these cells increased with increasing distance from the junction.

Hall-coefficient and resistivity measurements were used by RCA to investigate the crystal growth and irradiation-temperature dependence of the introduction rate and room-temperature annealing of carrier-removal defects in lithium-doped silicon. Initial resistivity of the quartz-crucible-grown silicon (QC) used in these studies was 30 ohm-cm and of the float-zone silicon was $\geq$1500 ohm-cm. The silicon was doped with lithium to a density of 2×10^{16} cm^{-3}. Irradiations were carried out with 1-MeV electrons at bombardment temperatures ranging from 79°K to 280°K. Specimens were annealed to 200°K, thereby, separating intrinsic and impurity defects. Introduction rates of carrier-removal defects were exponentially dependent on the reciprocal of temperature for both types of crystal, but the slopes and limiting temperature values differed. The slope of the carrier-removal rate versus reciprocal temperature curve was 0.055 eV in QC silicon and 0.09 eV in FZ silicon. The temperature-dependence was not consistent with a simple charge-state-dependent probability of interstitial-vacancy dissociation and impurity-vacancy trapping. Carrier concentrations measured at or near room temperature were increased in FZ silicon, but were decreased

in QC silicon by isothermal annealing at room temperature. QC silicon samples annealed to 373°K for 10 minutes exhibited complete recovery of mobility. Complete recovery of mobility in float-zone refined silicon took place in an annealing time $\leq$17 hours at room temperature. The time constant of the annealing kinetics at room temperature is consistent with the smaller lithium diffusion constant observed in oxygen-rich silicon compared to the lithium diffusion constant in oxygen-lean silicon. The mechanism of room-temperature annealing is attributed to neutralization of carrier-removal defects by lithium interaction in QC silicon, and by both lithium interaction and defect dissociation in FZ silicon. Results suggested that a lithium-oxygen-vacancy complex is produced by radiation in quartz-crucible grown silicon and a lithium-vacancy complex in float-zone refined silicon. The LiO-V defect is tightly bound compared to the oxygen-free Li-V defect. Measurements of carrier density as a function of reciprocal temperature located defect-energy levels near E_C-0.18 eV and E_C-0.13 eV, in irradiated-crucible silicon. The first defect level is the A-center and the latter is the reverse annealing center which is formed at a temperature of 250°K. A defect level located near E_C-0.08 eV formed after QC silicon samples were annealed at room temperature and lithium interacted with radiation defects.

The work during the latter part of the previous program consisted of measurement of the physical properties and photovoltaic performance of a large number of JPL-furnished cells before irradiation and after recent irradiation to fluences of 1×10^{14}, 5×10^{14}, and 3×10^{15} e/cm^2. A total of thirty-two crucible-grown cells, irradiated to 1×10^{14} e/cm^2, suffered no redegradation in a period extending to 69 days after irradiation. All cells except five (Lot C2) showed significant recovery, one group of five having higher power than n/p control cells irradiated to the same level. This group of cells (Lot C2) were initially doped with antimony before diffusion with lithium. A Lot of Lopex cells with very heavy lithium doping (Lot T3) subsequently suffered short-circuit current redegradation of approximately 5 percent in the period from the 20th to the 60th day after irradiation. Measurements on five batches of float-zone cells (Lot C4) with different lithium diffusion and redistribution schedules indicated a decrease in lithium density and increase in minority-carrier diffusion length and photovoltaic response with increasing redistribution time.

At the end of the previous program, the recommendations for producing stable, high-performance, high radiation-resistant lithium cells were: (1) to fabricate the cells from silicon of moderate resistivity (phosphorus-doped ~10 ohm-cm), (2) to diffuse lithium into the cell with a concentration of 3 to 10×10^{14}/cm^3 located at the edge of the depletion region, and (3) to distribute the lithium near

the junction such that the density gradient is $\approx 10^{19}$ cm^{-4}. The choice of oxygen content would depend on the rate of recovery required by the space mission in question.

SECTION II

LONG-TERM PERFORMANCE OF JPL-FURNISHED CELLS

A. GENERAL

In the previous contract, 5 shipments of lithium cells were received from JPL. The cells were manufactured by T.I., (T), Heliotek, (H) and Centralab (C) from a wide variety of silicon stock with varying lithium introduction conditions. Several competitive 10 ohm-cm n/p commercial solar cells were supplied for comparison purposes. Investigation of these cells has been carried over into the present contract. Tests performed on the cells included measurements of photovoltaic I-V characteristic under Tungsten illumination, p/n junction characteristics in the dark, reverse-bias capacitance characteristics, and minority-carrier diffusion length in the base region. Tungsten I-V characteristics were measured with a power density of 140 mW/cm^2 incident on the cell surface. Cell temperature was maintained at 28°C by water and forced-air cooling. These measurements have long term reproducibility of approximately 2 percent. In addition to the measurements at 140 mW/cm^2, comparative I-V characteristics were frequently taken at a number of light levels to provide information on cell series resistance and junction properties (Ref. 2). During the previous year cells of shipments No. 1, 2, and 3 had been irradiated at room temperature by 1-MeV electrons to one of three fluences:* 1×10^{14} e/cm^2, 5×10^{14} e/cm^2 or 3×10^{15} e/cm^2. At the start of the present reporting period cells from shipments No. 4 and 5 were irradiated to one of two fluences: 3×10^{14} e/cm^2 or 3×10^{15} e/cm^2. In the case of shipments No. 3, 4, and 5 several cells were left unirradiated for other experiments and to test the stability of unirradiated lithium cells.

A thorough discussion of the behavior of cells from shipments No. 1, 2, and 3 for post-irradiation times ranging from 76 days to 142 days was presented in the final report on the work of the previous year (Ref. 1). In the present report the most recent stability data on these cells, obtained during the present reporting period, will be presented and compared with the data which preceded it, i.e., the last data of last year's work. The present report contains our first post-irradiation data on the cells of shipments No. 4 and 5. Consequently, a separate discussion of these cells will be given.

---

*In one of the irradiations, due to an error, cells were exposed to $\approx 8 \times 10^{14}$ e/cm^2 of $\approx$70 MeV electrons instead of the intended 5×10^{14} e/cm^2 of 1-MeV electrons.

The cells of shipments No. 4 and 5, following the procedure used in the first three shipments, were divided and irradiated in groups. Three cells from each cell-lot of ten were irradiated to 3×10^{14} e/cm^2, e.g., groups C5(1), C5(3), three more were irradiated to 3×10^{15} e/cm^2, e.g., group C5(2), C5(4), and the remaining four were left unirradiated and retained for unirradiated stability studies and for experiments on the cold finger apparatus described elsewhere in this report.

B. CELLS OF SHIPMENTS NO. 1, 2, AND 3

Table I gives post-irradiation performance figures for the cell groups of shipments No. 1, 2, and 3. The first column gives the cell group code, where the letter identifies the manufacturer, the first number gives the cell lot and the number in parentheses gives the cell group within a given lot. The second and third columns give the silicon growth method (quartz-crucible, Lopex, float-zone) and n-type base dopant, respectively. The fourth and fifth columns give the donor density at the edge of the depletion region and the donor density gradient, both obtained from pre-irradiation capacitance-voltage measurements. The sixth column gives the electron fluence experienced by the cells. The seventh through tenth columns give the elapsed time after irradiation, averaged short-circuit current, power, and open-circuit voltage, respectively, as of the most recent reading. The eleventh through fourteenth columns give similar values for the previous reading. Individual cell groups will be discussed briefly.

The average initial (pre-irradiation) output for C1-cells was 30.6 mW which was higher than the 28.1 mW for n/p control cells. During irradiation to 1×10^{14} e/cm^2, C1(1) cells degraded in performance to P = 18.6 mW. These cells continue to experience slow recovery. As of the most recent set of readings, 283 days after irradiation, the power of C1(1) cells was 23.0 mW, approximately 8 percent above the 21.4-mW averaged power for four n/p cells irradiated to 1×10^{14} e/cm^2. Cells of group C1(2) degraded to P = 13.8 mW during irradiation to a fluence of $\approx 8 \times 10^{14}$ e/cm^2 of $\approx$0.7-MeV electrons. No significant recovery occurred during the first 76 days after irradiation, however, as of the 217th day the cells have recovered to a power of 14.8 mW, 10 percent below the 16.5 mW for n/p cells experiencing the same irradiation. These cells are still presumably recovering. The slow recovery in C1 cells is attributed to the low lithium density in these cells and to the high oxygen content of the cells (which has been found to lower the lithium diffusion constant in QC cells to a factor of ~1000 below that in FZ cells).

The QC grown, but more heavily doped H1 cells had low initial power, 20.7 mW. Group H1(1) cell recovery has evidently saturated at 20.2 mW. Group H1(2) cells continue to recover and 217 days after irradiation have power of 15.3 mW, approximately 7 percent below the n/p level.

TABLE I. PROPERTIES OF CELLS OF SHIPMENTS 1, 2, AND 3 AFTER IRRADIATION

No. of Cells in Group	Growth Method	Dopant	N_{LO} (cm^{-3})	dN_L/dw (cm^{-4})	Φ (e/cm^2)	LATEST READINGS				PREVIOUS READINGS			
						T.A.B.† (days)	I_{SC} (mA)	P_{MAX} (mW)	V_{OC} (mV)	T.A.B.† (days)	I_{SC} (mA)	P_{MAX} (mW)	V_{OC} (mV)
C1(1)	QC	As	$<10^{14}$	1×10^{18}	1×10^{14}	283	58.3	23.0	538	142	54.6	20.6	529
*C1(2)		As	$<10^{14}$	1×10^{18}	8×10^{14}	217	42.5	14.8	480	76	39.4	13.7	469
H1(1)		As	5×10^{14}	2×10^{19}	1×10^{14}	283	51.7	20.2	551	142	51.7	20.2	547
*H1(2)		As	5×10^{14}	2×10^{19}	8×10^{14}	217	41.7	15.3	513	76	40.1	14.4	504
C2(1)		Sb	?	?	1×10^{14}	280	47.8	18.8	519	139	46.6	17.9	517
C2(2)		Sb	?	?	5×10^{14}	217	40.6	14.9	486	76	40.6	14.9	486
C2(3)		Sb	?	?	3×10^{15}	217	31.2	10.9	451	76	31.2	10.9	451
H2(1)		P	5×10^{14}	1×10^{19}	1×10^{14}	280	57.5	23.1	556	142	57.5	23.1	556
H2(2)			5×10^{14}	1×10^{19}	5×10^{14}	217	50.2	19.4	525	76	46.1	17.4	511
H2(3)			5×10^{14}	1×10^{19}	3×10^{15}	217	41.2	13.8	469	76	34.8	11.6	462
T2(1)			2×10^{14}	1×10^{18}	1×10^{14}	280	61.8	23.4	559	139	62.5	23.4	559
T2(2)			2×10^{14}	1×10^{18}	5×10^{14}	217	58.5	20.2	525	76	58.5	20.2	525
T2(3)			2×10^{14}	1×10^{18}	3×10^{15}	217	series resistance				series resistance		
T3(1)	L		3×10^{15}	1×10^{20}	1×10^{14}	188	52.7	-	-		54.7	-	-
*T3(2)	L		3×10^{15}	1×10^{20}	8×10^{14}		42.4	-	-		43.4	-	-
T3(3)	L		3×10^{15}	1×10^{20}	3×10^{15}		38.3	14.0	534		39.3	14.2	532
batch I C4(1)	FZ		3×10^{15}	5×10^{19}	1×10^{14}		37.2	14.3	515		37.6	14.8	524
batch I C4(2)			3×10^{15}	5×10^{19}	5×10^{14}		36.9	13.9	510		37.9	14.4	523
batch I C4(3)			3×10^{15}	5×10^{19}	3×10^{15}		36.3	12.7	496		37.0	13.0	501
batch II C4(5)			2×10^{15}	2×10^{19}	1×10^{14}		42.5	16.2	516		43.2	17.0	526
batch II C4(6)			2×10^{15}	2×10^{19}	5×10^{14}		43.1	15.8	513		43.8	16.5	520
batch II C4(7)			2×10^{15}	2×10^{19}	3×10^{15}		43.0	14.3	491		44.1	14.1	486
batch III C4(9)			2×10^{14}	1×10^{18}	1×10^{14}		53.4	20.2	524		53.8	20.5	527
batch III C4(10)**			2×10^{14}	1×10^{18}	5×10^{14}		54.6	17.6	512		55.3	17.9	512
batch III C4(11)			2×10^{14}	1×10^{18}	3×10^{15}		49.7	6.0	429		47.2	5.7	422
batch IV C4(13)			2×10^{15}	2×10^{19}	1×10^{14}		37.8	13.4	500		38.0	14.2	515
batch IV C4(14)			2×10^{15}	2×10^{19}	5×10^{14}		37.6	13.9	503		38.0	14.4	518
batch IV C4(15)			2×10^{15}	2×10^{19}	3×10^{15}		36.8	13.2	497		37.3	13.3	500
batch V C4(17)			3×10^{14}	1×10^{18}	1×10^{14}		50.9	18.7	521		51.7	19.3	521
batch V C4(18)			3×10^{14}	1×10^{18}	5×10^{14}		51.7	19.1	519		52.3	19.1	520
batch V C4(19)			3×10^{14}	1×10^{18}	3×10^{15}		49.9	12.2	457		50.0	12.1	451

* irradiated with ≈ 0.7-MeV electrons
** series resistance developed after irradiation
† time after bombardment

Cells of Lot C2, the only lot tested which were made from antimony-doped silicon (QC) presented a puzzle in that no recovery had occurred as much as 139 days after irradiation. However, the most recent measurements show small but significant recovery in one of the three groups C2(1). Two hundred and eighty days after irradiation these cells, irradiated to 1×10^{14} e/cm^2, recovered in power from 17.9 to 18.8 mW. Two hundred and seventeen days after irradiation, groups C2(2) and C2(3) have not yet shown recovery. The cells of group H2(1) also had reasonably good initial performance (P_o = 26.0 mW). The recovery saturated sixty-nine days after irradiation, giving the H2(1) cells an averaged power of 22.9 mW, 7 percent above the average of two 10-ohm-cm n/p cells irradiated to the same fluence. The cells have been stable since that time.

The cells of group H2(2) had initial power of 24.3 mW; the H2(3) cells, 25.2 mW. Both groups continue to recover with H2(2) cells being 11 percent higher and H2(3) cells 3 percent lower in power than their respective n/p control cells.

The T2(1) and T2(2) cells, which had shown suspiciously fast recovery (Ref. 2) for QC grown cells have been stable between the latest two readings. They are superior in power output to their control cells by 10 percent and 14 percent, respectively. Cells of group T2(3) developed high series resistance after heavy irradiation to 3×10^{15} e/cm^2. This has been a problem encountered consistently by heavily irradiated lithium cells with a low level of base doping.

In reference to cells of lot T3, it was reported in the previous year's work that these cells had intermittent but severe shunt leakage (Ref. 1). This interpretation was in error, the leakage was caused by the picture-frame configuration of the cells together with the contacts used on the tungsten light table. The short-circuit current measurements, however, were not affected by this and thus are given for groups T2(1) and T2(2) in Table I. It can be seen that both groups suffered ≈4 percent redegradation in short-circuit current between the 76th and 188th day. Approximately 5 percent post-recovery redegradation had been suffered by these cells between the 10th and 76th day thus adding up to a total 9 percent redegradation in short-circuit current. Fortuitously, the cells of group T3(3) presented no contact problems and the photovoltaic characteristics were valid. These cells display the same behavior as the other two T3-groups. The instability in the T3 cells is attributed to their high lithium density and density gradient.

Cells of lot C4 came in 5 batches, indicated in Table I, the lithium diffusion schedule varying from batch to batch. Given in order of decreasing lithium density, the highest density first, they are: I, IV, II, V, III. Table I indicates that cells of all batches have suffered redegradation in short-circuit current ranging up to ≈3 percent in groups C4(3), batch I. A similar degradation was observed in all batches of unirradiated C4 cells.

In addition to the short-circuit current loss a ≈2 percent redegradation is observed in open-circuit voltage in the more lightly irradiated groups of the more heavily lithium doped cells, i.e., groups (1) and (2), batch I; groups (5) and (6), batch II; and groups (13) and (14) batch IV. In contrast, no significant voltage redegradation is seen either in the heavily irradiated groups from these batches or in any of the groups from the lightly doped batches III and V. Furthermore, a ≈2 percent voltage loss was suffered even in the unirradiated cells of the three heavily doped batches whereas none was observed in the two more lightly doped batches. This behavior is similar to that reported in earlier work (Ref. 3) where open-circuit voltage loss occurred when large amounts of free lithium exist near the junction. Evidently, a sufficiently high electron fluence can stabilize the cells by creating a sufficient number of defects to tie up a large fraction of the lithium.

C. CELLS OF SHIPMENT NO. 4

A total of 100 lithium cells was received in shipment No. 4. Forty of these cells, fabricated by Centralab (C5 series) represented an attempt to investigate the effects of two lithium diffusion techniques on QC and FZ cells. Ten of the forty cells supplied by T.I. (T5 series) were processed in the same manner as the T3 series previously received except that the T5 cells were processed as whole slices throughout all high temperature steps and sawed into individual cells only after contact sintering. Another 20 T.I. cells (groups T6 and T7) were processed using a long lithium diffusion time (480 minutes) at low temperature (325°C). The remaining cells were supplied by Heliotek. The Heliotek and Centralab cells were fabricated utilizing the lithium print-on technique and all the T.I. cells were made using evaporated lithium. Table II lists some process variables and properties of the cells in shipment No. 4 and also gives their initial photovoltaic characteristics. Sixty of these cells were irradiated on August 4, 1969, and packaged in dry ice (-78°C) until August 15, 1969, when their photovoltaic properties were measured. Each cell unavoidably remained at room temperature a total of approximately 15 minutes after irradiation before it could be measured. In addition, 4 control cells, furnished in shipment No. 3 (D-43, D-44, D-46, D-47), were irradiated with the cells from shipment No. 4. Table III gives the pre-irradiation and post-irradiation photovoltaic properties of these 10-ohm-cm n/p control cells.

The cells of group C5(1) had average initial output parameters of: I_O = 56.9 mA, P_O = 25 mW, and V_O = 599 mW, compared with that of the n/p control cell of I_O = 71.3 mA, P_O = 29 mW, and V_O = 554 mV. After irradiation to 3×10^{14} e/cm^2, the C5(1) cells degraded to I_O = 33.1 mA, P_O = 13 mW, V_O = 516 mV and their recovery history is given in Figure 1. Thirty-five days after bombardment the output power of the C5(1) group has increased to 19.9 mW or 80 percent of

TABLE II. GROUPING, IRRADIATION SCHEDULE PROCESS PARAMETERS LITHIUM CONCENTRATION AND INITIAL PHOTOVOLTAIC PROPERTIES OF C5, T4, H5, H6, T5, AND T7 CELLS

Cell Numbers	Cell Group	ϕ (e/cm^2)	ρ (Ω-cm)	Crystal Type	Dopant	Lithium Diffusion		Lithium Redistribution		Lithium Concentration		Diffusion Length L (μ)	I_o (mA)	P_o (mW)	V_o (mV)
						Time (min)	Temp (°C)	Time (min)	Temp (°C)	N_{LO} (cm^{-3})	$\frac{dN_L}{dw}$ (cm^{-4})				
C5-11, C5-12, C5-13	C5(1)	3×10^{14}	-	QC	-	40	450	0	0	1×10^{15}	7×10^{19}	35	56.9	25.0	599
C5-14, C5-15, C5-16	C5(2)	3×10^{15}	-	QC	-	40	450	0	0	1×10^{15}	4×10^{19}	40	58.1	25.1	598
C5-41, C5-42, C5-43	C5(3)	3×10^{14}	-	FZ	-	40	450	0	0	3×10^{15}	4×10^{19}	15	43.6	17.5	554
C5-44, C5-45, C5-46	C5(4)	3×10^{15}	-	FZ	-	40	450	0	0	2×10^{15}	2×10^{19}	15	41.9	15.8	547
C5-71, C5-72, C5-73	C5(5)	3×10^{14}	-	QC	-	90	425	120	425	2×10^{14}	1×10^{18}	115	71.9	30.9	595
C5-74, C5-75, C5-76	C5(6)	3×10^{15}	-	QC	-	90	425	120	425	2×10^{14}	1×10^{18}	90	67.1	28.4	583
C5-101, C5-102, C5-103	C5(7)	3×10^{14}	-	FZ	-	90	425	120	425	2×10^{14}	1×10^{18}	35	56.5	21.6	540
C5-104, C5-105, C5-106	C5(8)	3×10^{15}	-	FZ	-	90	425	120	425	2×10^{14}	1×10^{18}	40	57.9	20.8	532
T4-11, T4-12, T4-13	T4(1)	3×10^{14}	> 50	FZ	Phos	90	400	0	0	5×10^{15}	2×10^{20}	40	55.1	22.9	583
T4-14, T4-15, T4-16	T4(2)	3×10^{15}	> 50	FZ	Phos	90	400	0	0	5×10^{15}	3×10^{20}	50	56.7	22.3	580
H5-00, H5-01, H5-02	H5(1)	3×10^{14}	≈20	FZ	Phos	90	350	60	350	3×10^{14}	4×10^{16}	120	74.5	28.7	556
H5-04, H5-11, H5-13	H5(2)	3×10^{15}	≈20	FZ	Phos	90	350	60	350	3×10^{14}	2×10^{16}	125	71.5	27.0	557
H6-22, H6-27, H6-43	H6(1)	3×10^{14}	≈20	QC	Phos	90	450	60	450	-	-	45	60.3	24.7	577
H6-19, H6-28, H6-36	H6(2)	3×10^{15}	≈20	QC	Phos	90	450	60	450	5×10^{14}	1×10^{19}	30	50.6	20.9	550
T5-11, T5-12, T5-13	T5(1)	3×10^{14}	≈50	Lopex	Phos	90	400	0	0	6×10^{15}	3×10^{20}	80	58.9	25.2	597
T5-14, T5-15, T5-16	T5(2)	3×10^{15}	≈50	Lopex	Phos	90	400	0	0	6×10^{15}	4×10^{20}	50	55.1	23.4	596
T6-11, T6-12, T6-13	T6(1)	3×10^{14}	≥50	Lopex	Phos	480	325	0	0	1×10^{15}	3×10^{19}	115	69.2	26.8	594
T6-14, T6-15, T6-16	T6(2)	3×10^{15}	≥50	Lopex	Phos	480	325	0	0	1×10^{15}	3×10^{19}	140	69.6	25.4	589
T7-11, T7-12, T7-13	T7(1)	3×10^{14}	≥20	QC	Phos	480	325	0	0	2×10^{15}	5×10^{19}	110	70.8	25.2	587
T7-14, T7-15, T7-16	T7(2)	3×10^{15}	≥20	QC	Phos	480	325	0	0	1×10^{15}	3×10^{19}	-	70.5	25.1	581

TABLE III. PRE- AND POST-IRRADIATION PHOTOVOLTAIC PERFORMANCE OF N/P CONTROL CELLS

Control Cell	ϕ (e/cm^2)	Pre-Irradiation			Post-Irradiation			Post-Irradiation		
		I_o(mA)	P_o(mW)	V_o(mV)	I(mA)	P(mW)	V(mV)	(I/I_o)	(P/P_o)	(V/V_o)
D-43	3×10^{15}	68.6	27.8	552	42.4	14.5	475	0.62	0.52	0.86
D-44	3×10^{15}	71.7	29.0	555	42.1	14.2	470	0.59	0.49	0.85
D-45	3×10^{15}	70.4	28.2	553	42.2	13.9	470	0.60	0.49	0.85
D-46	3×10^{14}	70.2	27.0	547	54.7	19.1	505	0.78	0.71	0.92
D-47	3×10^{14}	71.3	29.0	554	54.6	19.9	505	0.77	0.69	0.91
D-48	3×10^{14}	68.8	28.6	569	52.7	19.5	510	0.77	0.68	0.90

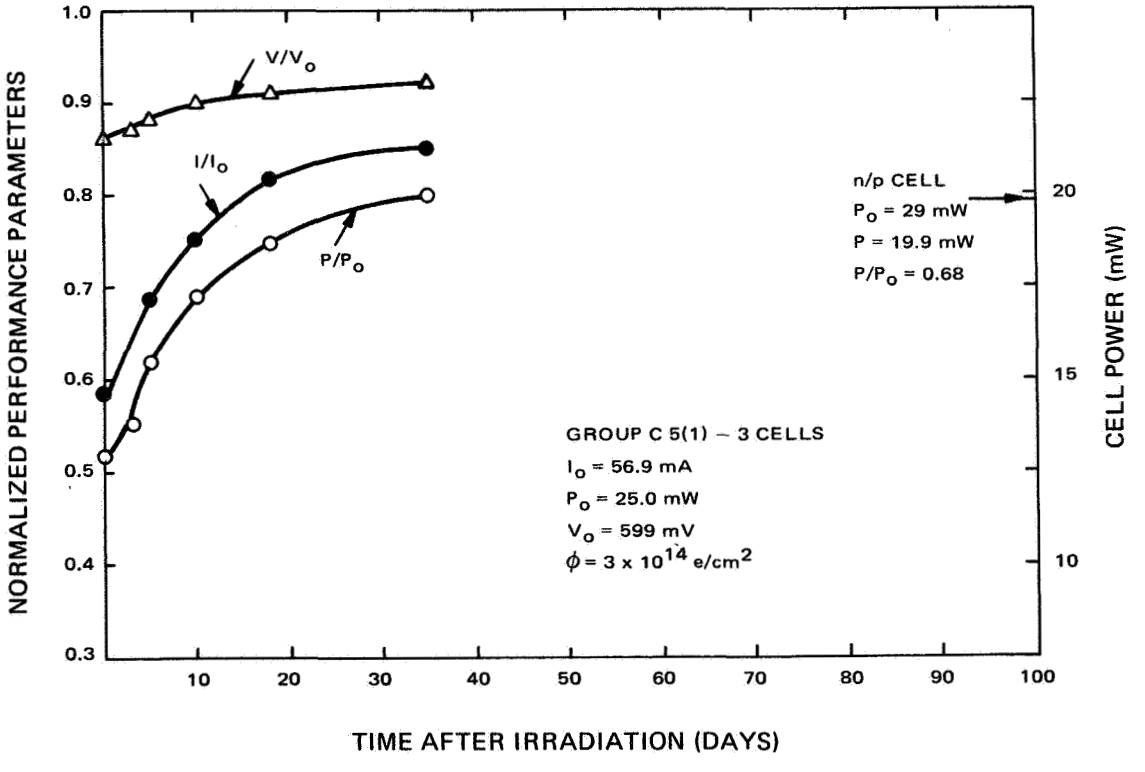

Figure 1. Cell Performance Vs. Time After Irradiation to 3×10^{14} e/cm^2 (1-MeV Electrons) - C5(1) Cells

their initial value and is equal to that power obtained from the control n/p cell irradiated with them (D-47). More recovery is expected of these cells in the future since the curve has not yet saturated. This rather rapid recovery for QC cells is believed due to the high lithium concentration present in these cells ($N_{LD} = 10^{15}\,cm^{-3}$, $dN_L/dw = 7 \times 10^{19}\,cm^{-4}$).

The average initial output parameters of group C5(2) cells were $I_O = 58.1$ mA, $P_O = 25.1$ mV, and $V_O = 598$ mV, while the control n/p cell (D-44) had the following performance parameter $I_O = 71.7$ mA, $P_O = 29$ mW, and $V_O = 555$ mV. C5(2) cells were irradiated to $3 \times 10^{15}\,e/cm^2$, have degraded to $I_O = 24.3$ mA, $P_O = 8.2$ mW, and $V_O = 459$ mV and are recovering at a linear rate, somewhat slower than the C5(1) cells due to the higher fluence (see Figure 2). After 35 days they are only 14 percent lower in output power (12.2 mW) than the n/p control cell (14.2 mW) irradiated with them, and much more recovery is expected of them.

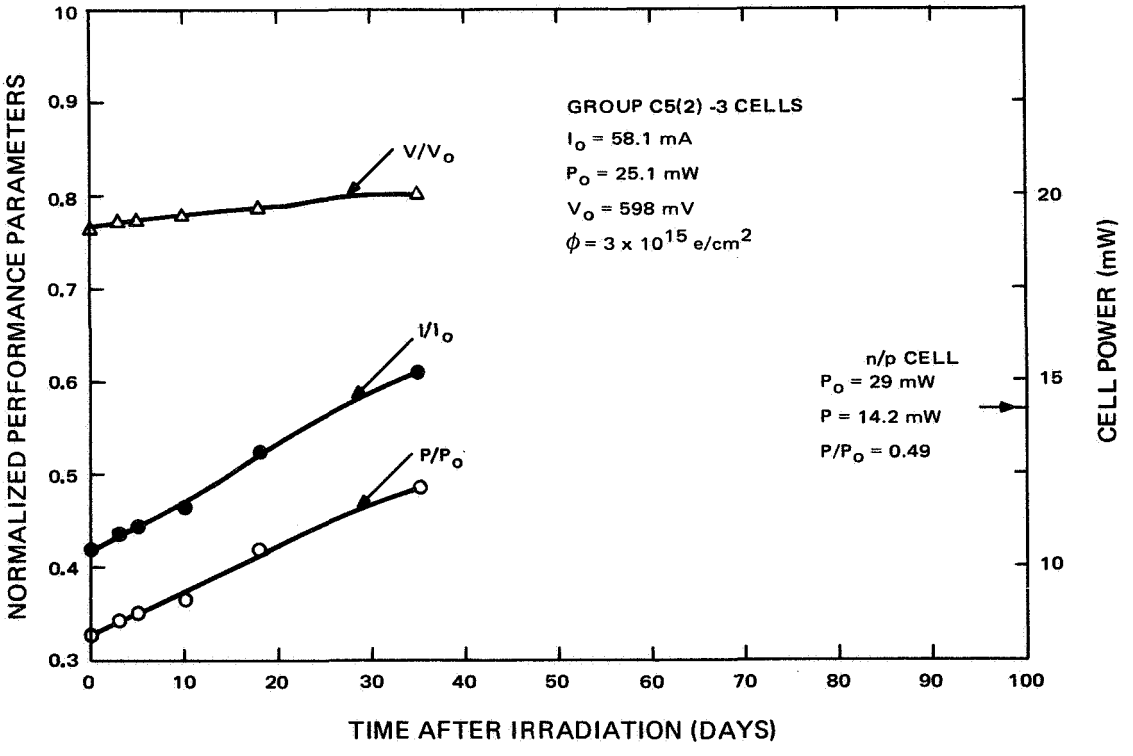

Figure 2. Cell Performance Vs. Time After Irradiation to $3 \times 10^{15}\,e/cm^2$ (1-MeV Electrons) - C5(2) Cells

Group C5(5) and C5(6) cells have shown no recovery of photovoltaic properties for 35 days after irradiation to 3×10^{14} e/cm^2 and 3×10^{15} e/cm^2, respectively. Their initial powers of 30.9 mW and 28.4 mW have been reduced to 16.6 mW and 11 mW, respectively, while the controls were lowered in power from 29 mW to 19.9 mW (D-47) and from 29 mW to 14.2 mW (D-44). These cells have been made from QC silicon as were the C5(1) and C5(3) cells, but have had a different lithium schedule than groups C5(1) and C5(3) resulting in a lower lithium density ($N_{LO} = 2 \times 10^{14}$ cm^{-3}, $dN_L/dw = 10^{18}$ cm^{-4}). It appears that the lithium diffusion and redistribution schedule yields too low a lithium density near the junction for significant short-term recovery to occur.

The C5(3) and C5(4) cells had significantly lower pre-irradiation performance values (17.5 mW and 15.8 mW) than the other C5 series cells. Upon irradiation to 3×10^{14} e/cm^2 and 3×10^{15} e/cm^2 these FZ cells decayed rather slightly ($P/P_0 = 0.76$, $P/P_0 = 0.61$) and recovered rather rapdily (three days) to 92 percent and 83.3 percent, respectively, of initial power and have stabilized these for the last 32 days. These groups now generate 16.1 mW and 13.2 mW, respectively, while the n/p controls give 19.9 mW (D-47) and 14.2 mW (D-44).

After an irradiation to 3×10^{14} e/cm^2, group C5(7) cells developed a series resistance of about 1.85 ohm (initial series resistance was ~0.75 ohm) probably due to carrier removal since the lithium density was rather low in these FZ cells. The cells have continued to recover in I_{SC}, V_{OC}, and P_{max} for the last 35 days but the series resistance has prevented the P_{max} from recovering to more than 0.755 P_O while I_{SC} and V_{OC} have recovered to 98 percent and 95 percent of initial values.

The cells of group C5(8), irradiated to 3×10^{15} e/cm^2 have developed a high enough series resistance to limit the short circuit current and their fourth quadrant I-V characteristics are straight lines. More detailed analysis of these cells will be given in the next reporting period.

FZ cells of group T4(1) irradiated to 3×10^{14} e/cm^2 have degraded from I_O = 55.1 mA, P_O = 22.9 mW, and V_O = 0.583 mV to I_O = 40.1 mA, P_O = 15.3 mW, and V_O = 0.532 mV, but recovered within about 3.5 hours to I_O = 49.3 mA, P_O = 19.5 mW, and V_O = 551 mV. Since that time these cells have redegraded to I_O = 46.8 mZ, P_O = 18.5 mW, and V_O = 561 mV and appear to be stabilizing there. At this point in time, 35 days after irradiation, the n/p control cell (D-46, P = 19.1 mW) and the T4(1) cells generate about the same output power. The T4(2) group of cells irradiated to 3×10^{15} e/cm^2 show a similar behavior as the T4(1) cells. For example, their average power degrades upon bombardment from 22.3 mW to 7.91 mW and reaches a peak in recovery of 13.6 mW 3 days later, after which they redegrade and appear to stabilize at 13.1 mW about 8 percent below the power output of the n/p control cell (D-44).

The H(5) series of FZ cells have shown little recovery after irradiation to 3×10^{14} e/cm^2 or 3×10^{15} e/cm^2. In the H5(1) group the maximum power has only recovered from 12.3 mW after bombardment to 13.4 mW, 35 days after bombardment (initially 28.7 mW) well below the control cell's power of 19.1 mW. The lithium density in these cells was rather low, $N_{LO} = 3 \times 10^{14}$ e/cm^3, and the density gradient was exceedingly small $dN_L/dw = <10^{18}$ indicating a very low lithium density in the bulk of the cell, probably accounting for the slight recovery.

QC grown H6 cells have behaved rather predictably. The H6(1) group irradiated to 3×10^{14} e/cm^2 show linear recovery up to 35 days with an output of 17.5 mW, up from 14 mW after bombardment, while the control cell generates 19.1 mW. Group H6(2) irradiated to the higher fluence of 3×10^{15} e/cm^2 have not shown recovery to date (35 days after bombardment), but are expected to improve at a later date. The lithium density in both cell groups is of the order of 7×10^{14} cm^3.

Group T5 cells processed similarly as T3 cells except for the final slicing into individual cells behaved similarly to the T3 cells. This suggests that if any nonuniform lithium distribution exists at the cell edges (for cells sliced before any high temperature processing), the cell's performance is not affected by it. Group T5(1) cells irradiated to 3×10^{14} e/cm^2 recover very rapidly ($P_{max} = 11.1$ mW after bombardment and $P_{max} = 20.2$ mW, 3.5 hours later) and they redegrade gradually as shown in Figure 3. T5 (2) cells behave quite similarly.

Lopex cells of group T6(1) recover rather rapidly during the first three days following bombardment and appear to saturate after that. From an initial power of 26.8 mW, these cells recover to 20.7 mW in 3 days, 8 percent higher than the D-46 control cell. A shunt resistance inherent in the contacting structure when testing the T6(2) cells prevented accurate V_{OC} and P_{max} recovery measurements. However, I_{SC} measurements, not affected by shunt resistance, show a slower recovery as expected for T6(2) cells than T6(1) cells. In particular I_{SC} degraded from 69.6 mA to 24.5 mA after bombardment. Thirty-five days later, the short circuit current was measured at 47.4 mA. In comparison the n/p control cell measures 42.4 mA short circuit current.

The QC grown cells of group T7(1) have recovered rather rapidly from 10.8 mW after irradiation to 3×10^{14} e/cm^2 to 19.4 mW, 3 days after irradiation (same power level as control cell). Although these cells have a moderately high lithium density ($N_{LD} = 1.5 \times 10^{15}$/cm^3) and gradient ($dN_L/dw = 4.7 \times 10^{19}$/cm^4) their recovery is fast for QC type cells. In addition, they do degrade (about 3 percent) after 3 days and kind of stabilize, much like the T6 cells. The T7(2) cells also closely follow the recovery record of the T6 Lopex cells. It appears then, that at least in a preliminary way, these QC cells behave analogously to cells with lower oxygen content than that usually present in crucible material.

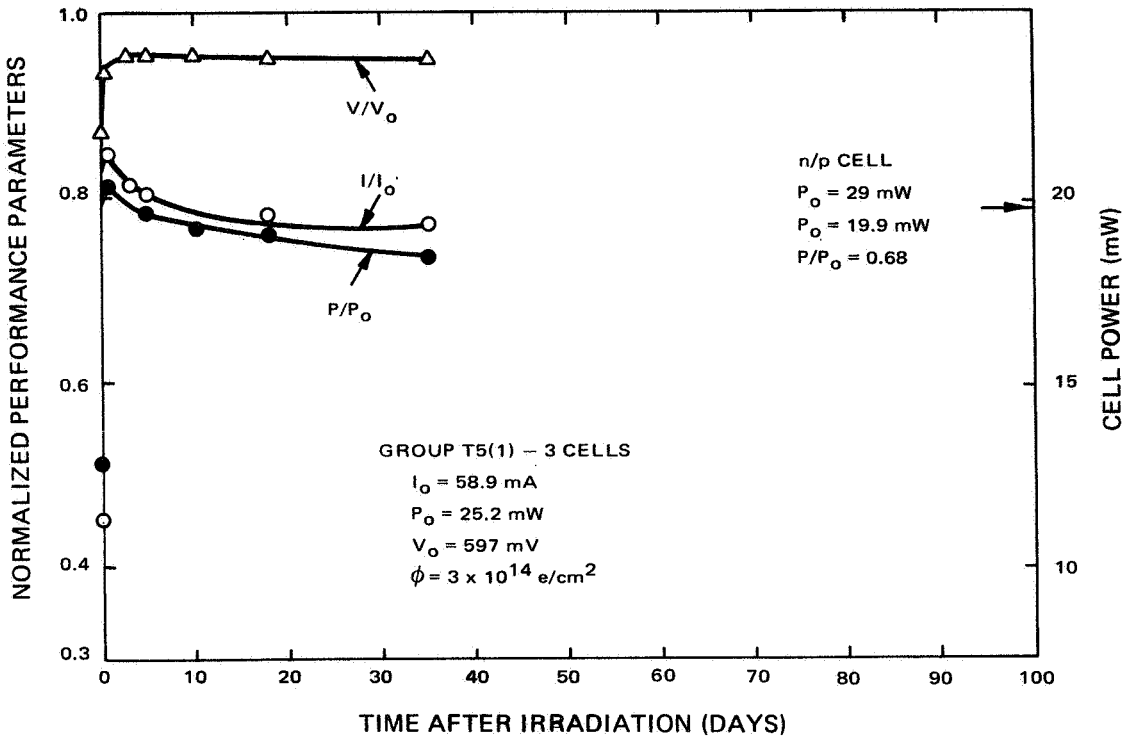

Figure 3. Cell Performance Vs. Time After Irradiation to 3×10^{14} e/cm^2 (1-MeV Electrons) - T5(1) Cells

D. CELLS OF SHIPMENT NO. 5

Fifty lithium cells were received in this shipment and thirty of these were irradiated on August 4, 1969, along with cells from shipment No. 4 and two control cells (D-45, D-48). These thirty cells were kept in dry ice (except for about 15 minutes at room temperature) with shipment No. 4 cells before photovoltaic measurements were made. Table IV lists the process parameters and initial photovoltaic properties of the cells irradiated from this shipment. The C6A and C6B group of cells from Centralab were antimony doped while group C6C cells were phosphorus doped. None of these cells has shown any recovery as of 35 days after irradiation. This is not too surprising though for QC grown cells with doping densities in the 10^{14}/cm^3 range and gradients of 10^{18}/cm^4 as measured in the C6A, C6B, and C6C groups.

Lopex cells from group H7(1) recover rapidly (several hours) to about 90 percent of their initial power after an irradiation of 3×10^{14} e/cm^2 and quickly saturate. As of 35 days after irradiation their photovoltaic properties are I = 52.1 mA, I/I_O = 91.4 mV, V = 551 mV, V/V_O = 0.97, P = 21.5 mW, P/P_O = 0.89. The control cell (D-48) measures I = 52.7 mW, I/I_O = 0.77, V = 510 mV, V/V_O = 0.90, P = 19.5 mW, and P/P_O = 0.68. H7(2) cells recover slower than H7(1) cells as expected because of the 3×10^{15} e/cm^2 fluence, but still begin to saturate in recovery after only 5 days, with their output power being 14.7 mW as compared with 13.9 mW for the control.

TABLE IV. GROUPING, IRRADIATION SCHEDULE PROCESS PARAMETERS LITHIUM CONCENTRATION AND INITIAL PHOTOVOLTAIC PROPERTIES OF C6, H7, AND T8 CELLS

Cell Number	Cell Group	ϕ (e/cm^2)	ρ (Ω-cm)	Crystal Type	Dopant	Lithium Diffusion		Lithium Redistribution		Lithium Concentration		Diffusion Length L (μ)	I_0 (mA)	P_0 (mW)	V_0 (mV)
						Time (min)	Temp (°C)	Time (min)	Temp (° C)	N_{LO} (cm^{-3})	$\frac{dN_L}{dw}$ (cm^{-4})				
C6A-11	C6A(1)	3×10^{14}	3-16	QC	Antimony	90	425	120	425	5×10^{14}	1×10^{18}	110	66.7	28,2	584
C6A-12										1×10^{15}	2×10^{18}				
C6A-13										4×10^{14}	2×10^{18}				
C6A-14	C6A(2)	3×10^{15}	3-16	QC	Antimony	90	425	120	425	1×10^{15}	1×10^{18}	135	69.1	28.9	586
C6A-15										8×10^{14}	2×10^{18}				
C6A-16										4×10^{14}	1×10^{18}				
C6B-11, C6B-12, C6B-13	C6B(1)	3×10^{14}	17-85	QC	Antimony	90	425	120	425	—	—	130	66.7	29.3	592
C6B-14, C6B-15, C6B-16	C6B(2)	3×10^{15}	17-85	QC	Antimony	90	425	120	425	3×10^{14}	1×10^{18}	140	66.7	28.9	592
C6C-11, C6C-12, C6C-13	C6C(1)	3×10^{14}	16-57	QC	Phos.	90	425	120	425	3×10^{14}	1×10^{18}	100	68.5	28.1	584
C6C-14, C6C-15, C6C-16	C6C(2)	3×10^{15}	16-57	QC	Phos.	90	425	120	425	3×10^{14}	1×10^{18}	120	68.2	28.3	583
H7-82, H7-86, H7-88	H7(1)	3×10^{14}	20	Lopex	Phos.	90	425	60	425	—	—	25	57.1	24.1	569
H7-90, H7-91, H7-92	H7(2)	3×10^{15}	20	Lopex	Phos.	90	425	60	425	—	—	40	57.0	22.8	564
T8-11, T8-12, T8-13	T8(1)	3×10^{14}	>20	QC	Phos.	480	325	0	0	—	—	110	64.5	26.1	595
T8-14, T8-15, T8-16	T8(2)	3×10^{15}	>20	QC	Phos.	480	325	0	0	—	—	120	64.3	26.1	595

Group T8 cells apparently fabricated and processed like T7 cells except for the possible time of cell slicing (i.e., before or after high temperature processing) behave quite differently than the T7 cells. T8(1) cells had initial photovoltaic properties of I_o = 64.5 mA, P_o = 26.1 mW, and V_o = 595 mV and decayed to I = 36.8 mA, P = 12.6 mW, and V = 494 mV after irradiation to 3×10^{14} e/cm^2. These cells did not recover at all for 10 days showing typical QC cell behavior unlike T7 cells. Thirty-five days after irradiation, the T8(1) group has now recovered to I = 39.2 mA, P = 13.9 mW, and V = 502 mV and much more recovery is expected. The T8(2) group irradiated to 3×10^{15} e/cm^2 have not shown any recovery for thirty-five days, not unexpected for QC type cells.

E. ANOMALIES

Two noteworthy instances of anomalous behavior have been observed in the course of the experiments. The first concerns the forward dark I-V characteristics of some of the cells from Lots H5, T2, T3, T5, T6, T7, and T8. Somewhere in the vicinity of 20 mA forward diode current and 0.6 V forward bias the characteristic breaks sharply into an approximately linear region with very high series resistance, ~20 ohm. No explanation for this phenomenon, which has not been present in the light generated curves, has been found.

The second anomaly concerns the post-irradiation behavior of the 10 ohm-cm n/p control cells. Measurements indicate a ≈6 percent recovery in short circuit current from the immediate post-irradiation value over a period of six months with the cells at room temperature. It is not due to reproducibility problems since seven unirradiated controls from the same lot (D) were measured throughout this period and maintained a photovoltaic characteristic reproducible to within one percent.

SECTION III

SOLAR CELL EXPERIMENTS AT LOW TEMPERATURE

A. GENERAL

During the previous contract performed by RCA-AED for JPL (1968-1969), a cold finger apparatus for testing solar cells was designed and fabricated. This apparatus, which was previously described in detail (Ref. 1), can accommodate two devices with dimensions of approximately 0.13 × 0.30 inch. Heaters on the cold finger make possible testing between liquid nitrogen temperature (77°K) and the melting temperature (~380°K) of the solder used to mount the cells to the finger. The heaters are capable of raising the cell temperature from 77°K to 380°K in approximately one minute.

The principal cold-finger experiments are being made with the apparatus attached to the output flange of a 1-MeV Van de Graaff generator. Measurements of diffusion length by the electron voltaic method (Ref. 4) using the electron beam from this generator are taken for a series of electron irradiations and cell temperatures. In addition, forward and reverse (dark) diode characteristics and reverse-bias capacitance measurements can be made.

Two solenoid actuated rods entering the cold finger apparatus through a vacuum quick-connect enable automatic positioning of a 0.085-inch thick aluminum beam stop (for cell protection) or a 0.011-inch thick beam moderator (for diffusion length measurements, see Ref. 4) in front of the test cells. The bottom edge of the cold finger is directly on the beam axis of the Van de Graaff generator. Immediately behind and below the cold finger is a Faraday cup which monitors the electron beam current continuously.

B. EXPERIMENTAL DETAILS

The experiments of this reporting period were performed on two cells from Lot C6A. These cells are QC-grown cells with antimony doping to starting resistivities of 3 to 16 ohm-cm which were lithium-doped with a 90-minute diffusion at 425°C followed by a 120-minute redistribution at 425°C. Previous results on antimony-doped cells (Lot C2) were puzzling in that the cells failed to show significant recovery at room temperature, although the most recent measurements (Section II) show a small amount of room temperature recovery. Since there are significant variations in starting (Sb) resistivity within the cells of Lot C6A it was possible to choose two cells with significantly different doping densities.

The donor-density profiles obtained from capacitance-voltage plots, shown in Figure 4, indicated that cell C6A-19 was much more heavily doped than C6A-18. It is reasonable to assume that the donor-density difference reflects a difference in the Sb doping level rather than the Li doping level since both cells experienced identical Li-diffusion schedules, and since both cells have similar density gradients. These two cells were consequently chosen for the first cold finger experiments with the purpose of obtaining information on possible effects of the Sb dopant on recovery characteristics.

To make the cells compatible with size limitations of the cold finger, they were cut into 0.13 x 0.30 inch pieces. In order to minimize surface effects, the cells were cut by scribing the back surface and then cleaving. After cleaving, the cells' capacitance-voltage and diode characteristics were measured to check that no major changes occurred in the cutting process. The cells were then soldered onto a 0.020-inch thick metallized boron nitride wafer with Cerroseal (220°F) solder. The boron nitride wafer was bonded to the cold finger with Dow Corning silicon adhesive. Cell temperature was measured by a copper-constantan thermocouple permanently mounted on a dummy cell next to the test cells. The dummy cell mounting to the cold finger is identical to that of the test cells.

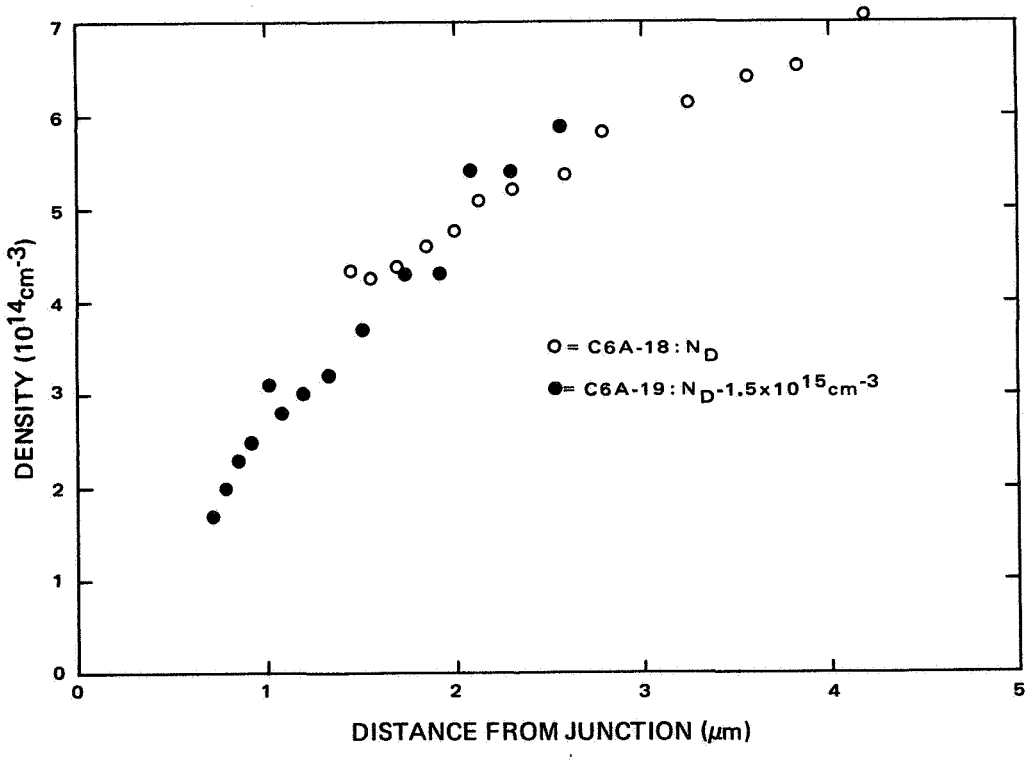

Figure 4. Donor Density Profiles for Cells C6A-18 and C6A-19

The cold finger experiments consisted of irradiations at ~77°K by 1-MeV electrons to fluences from 3×10^{13} e/cm^2 to 3×10^{15} e/cm^2 and anneals at room temperature and 373°K, with measurements of electron-voltaic short-circuit curent, capacitance-voltage, and diode characteristics at various stages of cell irradiation and annealing. From the short-circuit current the minority carrier diffusion length, L, was obtained using the method of Rosenzweig (Ref. 4).* Minority carrier lifetime, τ_0, was then obtained from the relation $\tau_0 = L^2/D$, where D is the minority-carrier diffusion constant. Values for D were obtained by use of the mobility data of Morin and Maita (Ref. 5) and application of the Einstein Relation. The experimental uncertainty in the short-circuit current measurement is approximately 10 percent giving an approximate 20-percent uncertainty in τ_0 assuming the values for D are correct. This latter assumption is considered valid for temperatures greater than ~140°K ($10^3/T \approx 7.1$). Below 140°K impurity scattering becomes significant leading to uncertainties in the value of D.

Recombination levels can be found by obtaining lifetime-temperature (τ vs T) plots and applying Hall-Shockley-Read analysis (Ref. 6 and 7). For n-type material the equations are (Ref. 8)

$$\tau_0 / \tau_{p0} = (1 + n_1/n_0), \tag{1}$$

or

$$\tau_0 / \tau_{p0} = (1 + \gamma\, p_1/n_0), \tag{2}$$

where

n_0 and p_0 are the thermal equilibrium electron and hole concentrations,

τ_{p0} is the minority-carrier (hole) lifetime when the Fermi level is near the conduction band,

γ is the ratio of the hole capture cross-section to the electron capture cross-section, and

n_1 and p_1 are the (ficticious) electron and hole concentrations which would exist if the Fermi level was located at the recombination level E_t.

Thus, $n_1 = N_c \exp [e (E_t - E_c) /kT]$, $p_1 = N_v \exp [e (E_v - E_t) /kT]$, where $N_c = N_v = 4.82 \times 10^{15} T^{3/2}$, E_C and E_V are the energy levels at the edge of the conduction and valence band, respectively. Equation (1) applies if the recombination level is in the upper half of the band gap; Equation (2) if the level is in the lower half. The value of n_0 to be used in these equations is the donor density obtained

---

* The beam current was sufficiently low that $\Delta n/n_0 < 10^{-5}$ in all measurements.

from C-V measurements. The large density gradients in lithium cells provide an uncertainty in that no single value of n_0 is applicable over the current collection volume in the short-circuit current measurements (i.e., over a diffusion length). However the uncertainty, $\triangle E$, introduced by the variation in n_0 can be approximated by the shift in Fermi level associated with this variation, that is

$$\triangle E_F \simeq \frac{kT}{e} \ln \frac{n_{02}}{n_{01}}, \tag{3}$$

where n_{01} and n_{02} are the lower and upper limits of n_0. For the present cells, the gradient near the junction is rather shallow, $\sim 10^{18} cm^{-4}$, giving $2 \lesssim n_{02}/n_{01} \lesssim 3$ which gives $\triangle E_F \sim kT/e$. Consequently, for the temperature range of the measurements this uncertainty is $\sim 0.02V$.

C. EXPERIMENTAL RESULTS

Before mounting on the cold finger, the cells were cut into 0.13×0.30 inch pieces which were numbered, and the pieces of each cell with the best I-V characteristics were chosen for mounting. These were designated cell No. C6A-18(2) and C6A-19(2).

Cells C6A-18(2) and C6A-19(2) were irradiated sequentially to fluences of 3×10^{13}, 3.3×10^{14}, 1.53×10^{15}, and $3 \times 10^{15} e/cm^2$ at $\approx 77°K$. During each irradiation, τ_0 was measured at closely spaced fluence intervals. After each irradiation, a ≈ 10 minute, 200°K anneal was performed to remove all divacancies (Ref. 9), then a τ_0 vs T plot was made. A ≈ 12 hour room temperature anneal also followed the irradiations to fluences of 3.3×10^{14}, 1.53×10^{15}, and $3 \times 10^{15} e/cm^2$. After the irradiation to $3 \times 10^{15} e/cm^2$, a 6-hour anneal at 373°K was performed, and τ_0 vs time at 373°K was measured to investigate cell recovery dynamics.

The results of the τ_0 vs T_M measurements are shown in Figures 5 and 6 on semi-log plots with $10^3/T_M$ as the abcissa. As stated previously, after each irradiation and before the τ_0 vs T_M curves were taken, 200°K anneals of ≈ 10 minutes duration were made to anneal out the divacancy defects formed during irradiation. To monitor completion of this annealing stage, measurements of τ_0 were made each minute at 200°K until saturation was achieved. The curves in Figures 5 and 6 indicated a recombination level somewhere in the vicinity of the $E_C - 0.185V$ level previously identified as the oxygen-vacancy or A-center (Ref. 9-11) in QC grown n-type silicon and more recently found at RCA (Ref. 1 and 12) in lithium doped QC-grown silicon samples.

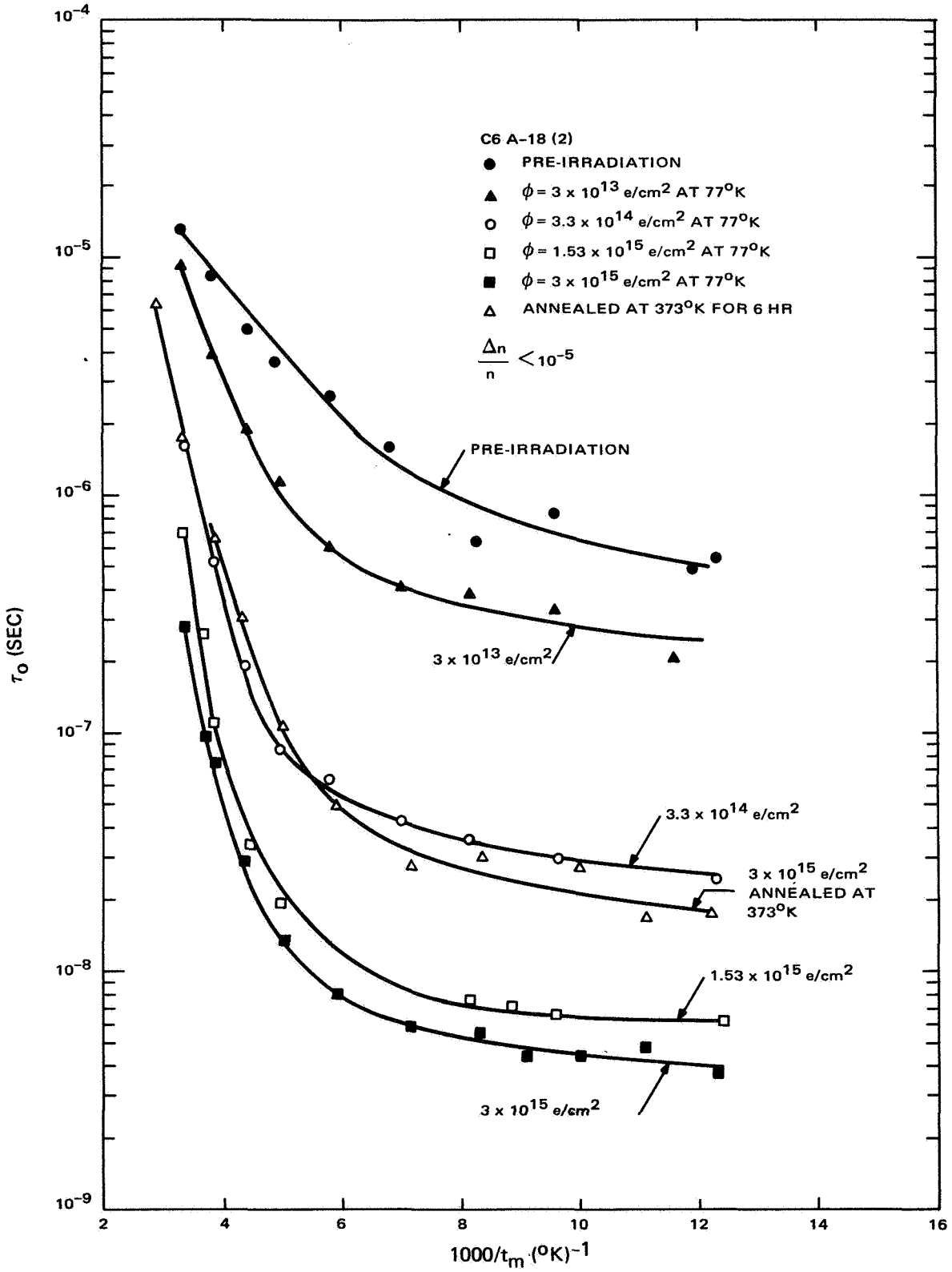

Figure 5. Lifetime vs Temperature Data on Cell C6A-18(2)

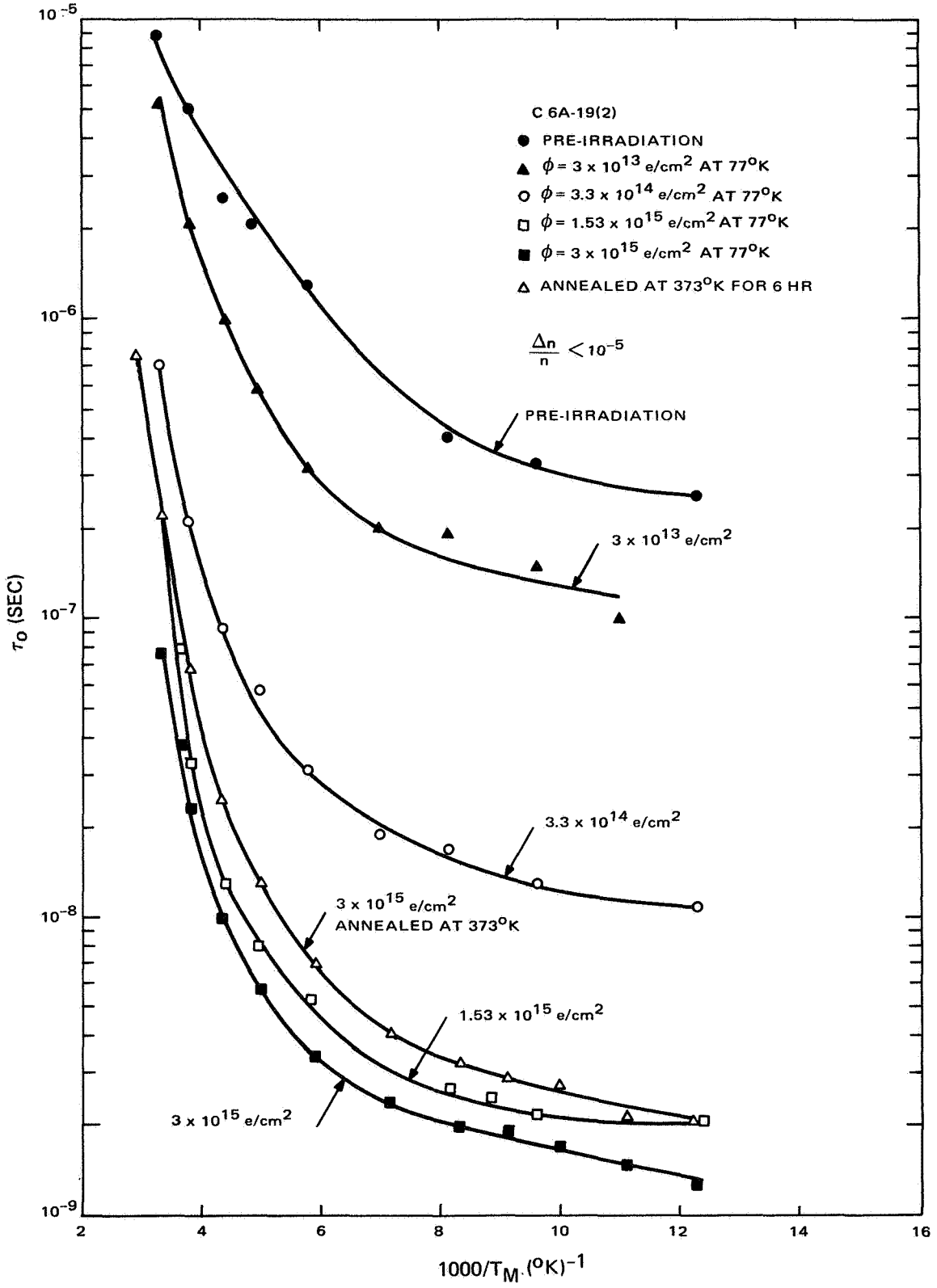

Figure 6. Lifetime vs Temperature Data on Cell C6A-19(2)

In Figures 7 and 8, theoretical curves of τ_0/τ_{p0} from Equation (1) are given, together with the experimental data taken after fluences of 3.3×10^{14} and 3×10^{15} e/cm^2 and after the 6-hour, 373°K anneal. Curve fitting was done only for temperatures of 140°K and above for two reasons: (1) impurity scattering becomes a factor below ≈140°K increasing the uncertainty in mobility (or D) value, and (2) the experimental value of τ_0 begins to increase significantly at temperatures slightly above 140°K. These reasons also dictated the choice of τ_{p0} to be the value of τ_0 at 140°K.

For cell C6A-18(2) shown in Figure 7 a value of $n_0 = 1 \times 10^{15}$ cm^{-3} was chosen with reference to Figure 4. The data of both post-irradiation experiments and the post-anneal data fit well within the envelope: $0.15\ V \leq E_C - E_T \leq 0.17\ V$ with the post-irradiation values fitting best the $E_C - E_T = 0.16$ V curve and the post-anneal data fitting best the $E_C - E_T = 0.15$ V curve. For cell C6A-19(2), the more heavily doped cell, $n_0 = 2 \times 10^{15}$ cm^{-3} was used to generate the theoretical curves from Equation (1). For this cell, Figure 8 shows the data to fit between $0.13\ V \leq E_C - E_T \leq 0.15$ V. Again for this cell the post-anneal level of 0.14 V is shallower than the post-irradiation level of 0.15 V. Even though the experimental uncertainty in the level is greater than the ≈0.01 V change which occurred during 373°K annealing cycle, the consistency of this change in both cells indicates that perhaps some reordering or perturbation of the level occurs during the 373°K anneal. Another possibility, however, is that a change in relative density of two closely spaced levels occurs during annealing. Such a distinction would not be observable in these measurements.

A puzzling feature of the results is the apparent ≈0.01 V difference in recombination level between cells C6A-18(2) and C6A-19(2). No basic differences should exist between these cells to cause such a difference and no statisfactory explanation has been found except a possible error in the choice of n_0 in Equation (1). If a value of $n_0 = 2 \times 10^{15}$ cm^{-3} were chosen for C6A-18(2), the levels would equal those obtained for C6A-19(2). Another question arises concerning the relation of the level found here to the A-center. Since the C6A cells are crucible-grown the expectation is that the main defect would be the A-center at $\approx E_C - 0.18$ V. The ≈0.02 V shallower level found in these experiments could be due to (1) measurement uncertainty, (2) perturbation of the level by the presence of lithium or antimony, or (3) the additional presence of another level close to the A-center level. The first and third of these possibilities seem more likely than the second. It is hoped that the next cold finger experiment, which will be made with a C6B-cell (lightly Sb doped) and a C6C-cell (P doped) will provide answers to some of these questions.

Cell lifetime was also measured during the cell irradiation. Since the irradiation temperature was 77°K, the lifetimes were also taken at 77°K. An uncertainty in mobility values of approximately 30 percent exists at this temperature, and,

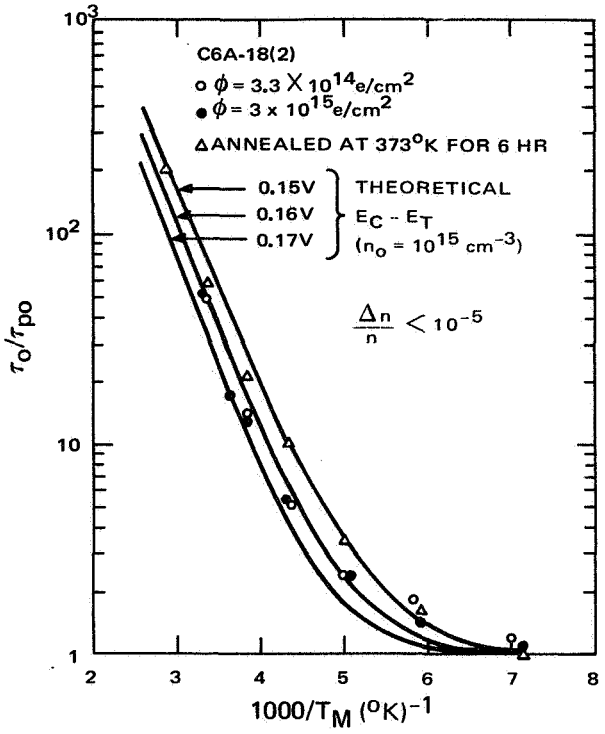

Figure 7. Theoretical and Experimental Lifetime vs Temperature Curves C6A-18 (2)

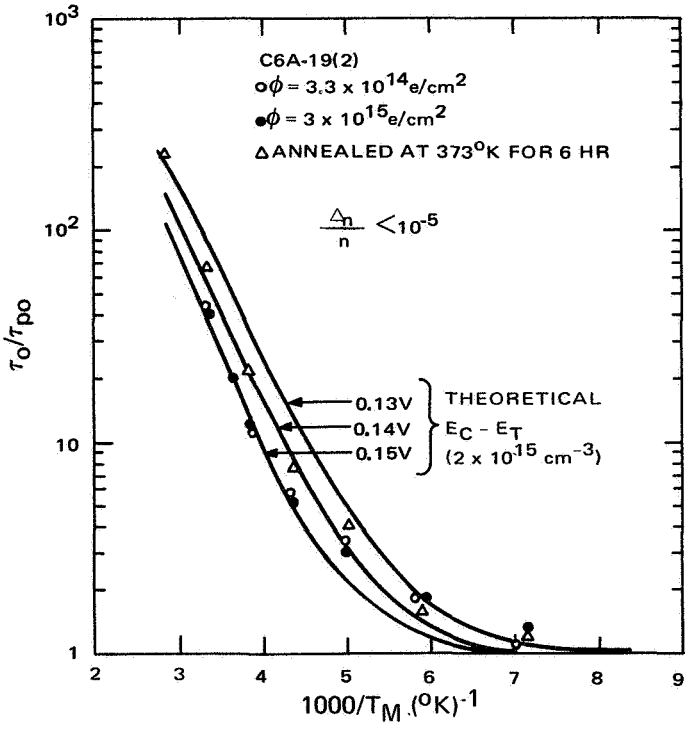

Figure 8. Theoretical and Experimental Lifetime vs Temperature Curves C6A-19(2)

therefore, the absolute lifetime values also include this added uncertainity since they were obtained from the equation $\tau = L^2/D$. However, since the fluence was kept below the threshold for significant carrier removal, the value of D at 77°K was constant throughout the experiment and the relative values are correct to within the accuracy of the diffusion-length measurement. In addition, the lifetime measurements were made at a higher beam current ($\approx 4 \times 10^{-8}$ A/cm^2) than the measurements of τ_0 vs T_n, made at $\approx 10^{-9}$ A/cm^2. However, even at 4×10^{-8} A/cm^2 the injection level ($\Delta n \approx 10^{10}$ cm^{-3} giving $\Delta n/n_o \lesssim 10^{-5}$) is very low so that $\tau = \tau_0$, the equilibrium lifetime. Comparison between computed lifetimes at the two beam current levels confirmed this.

Figure 9 gives logarithmic plots of lifetime vs fluence, Φ, for both cells. Since the measurements for any single irradiation were taken below the divacancy annealing temperature they reflect the damage introduction due to divacancies in addition to that due to other defects. The discontinuities in the curves at 3×10^{13}, 3.3×10^{14}, and 1.53×10^{15} e/cm^2 reflect the divacancy anneal plus (in the case of the latter two) a small amount of annealing at room temperature. The fluence dependence for both cells is the same; for $\Phi \gtrsim 10^{13}$ e/cm^2 an equation of the form

$$\frac{1}{\tau} = K\Phi^A \qquad (4)$$

fits well to the data, with a value of A of approximately 1.3.

After irradiation to a fluence of 3×10^{15} e/cm^2, a 6-hour anneal was performed at 373°K for the purpose of obtaining information on the annealing kinetics of the cells. Plots of minority-carrier lifetime at 373°K vs annealing time at 373°K are given in Figure 10. After an initial period of approximately 30 minutes for C6A-18(2) and approximately 80 minutes for C6A-19(2) in which a small decrease in lifetime is experienced, both cells began to recover. The recovery was particularly pronounced in C6A-18(2). An annealing stage at 400°K in phosphorus doped FZ silicon has previously been identified as the dissociation of the phosphorus-vacancy or E-center (Ref. 13). The analog of this center in the Sb-doped C6A cells would be the antimony-vacancy defect. Thus, the question arises as to whether we are observing the dissociation of antimony-vacancy defects during the 373°K anneal. This appears highly unlikely since the position of of the Sb-V center is at $\approx E_C - 0.4$ V (Ref. 14) would render it unobservable in these measurements. (Much higher measurement temperatures would be required to drive the Fermi level down to $E_C - 0.4$ V.) Also, if this were S_b-V dissociation, the annealing in the more havily Sb-doped cell (C6A-19(2)) should be more pronounced than in C6A-18(2). Figure 10 shows just the reverse to be true, i.e., the more than C6A-19(2).

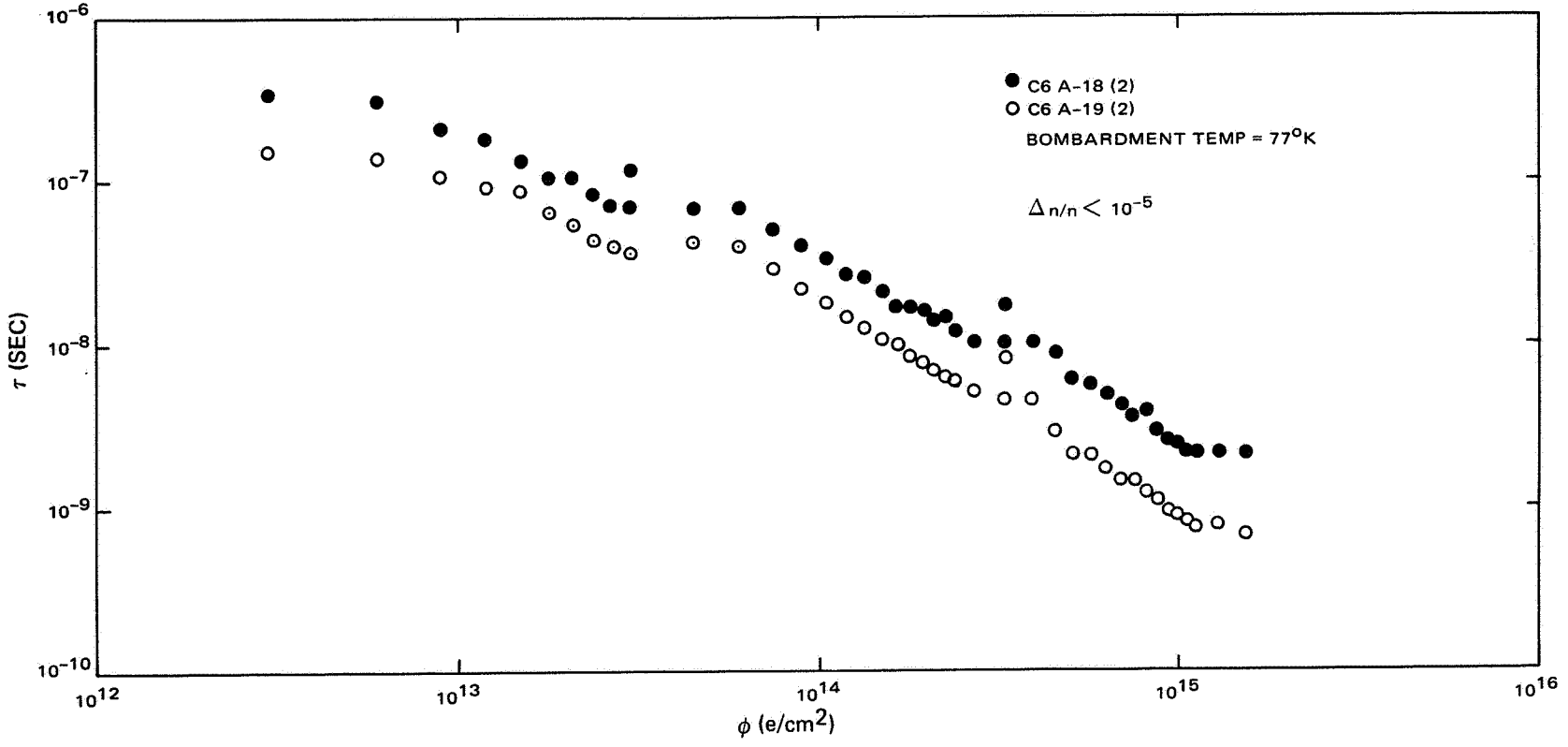

Figure 9. Lifetime vs Fluence Data-Cells C6A-18(2) and C6A-19(2)

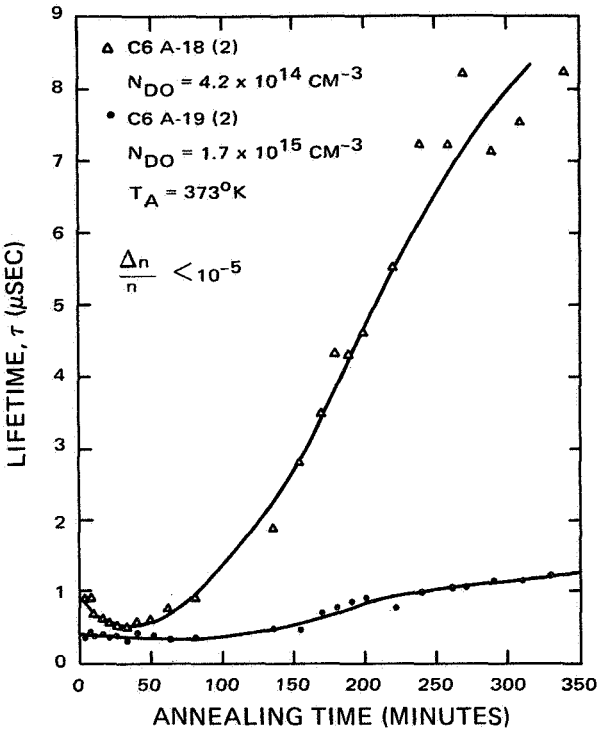

Figure 10. Lifetime at 373°K vs Annealing Time at 373°K-Cells C6A-18(2) and C6A-19(2)

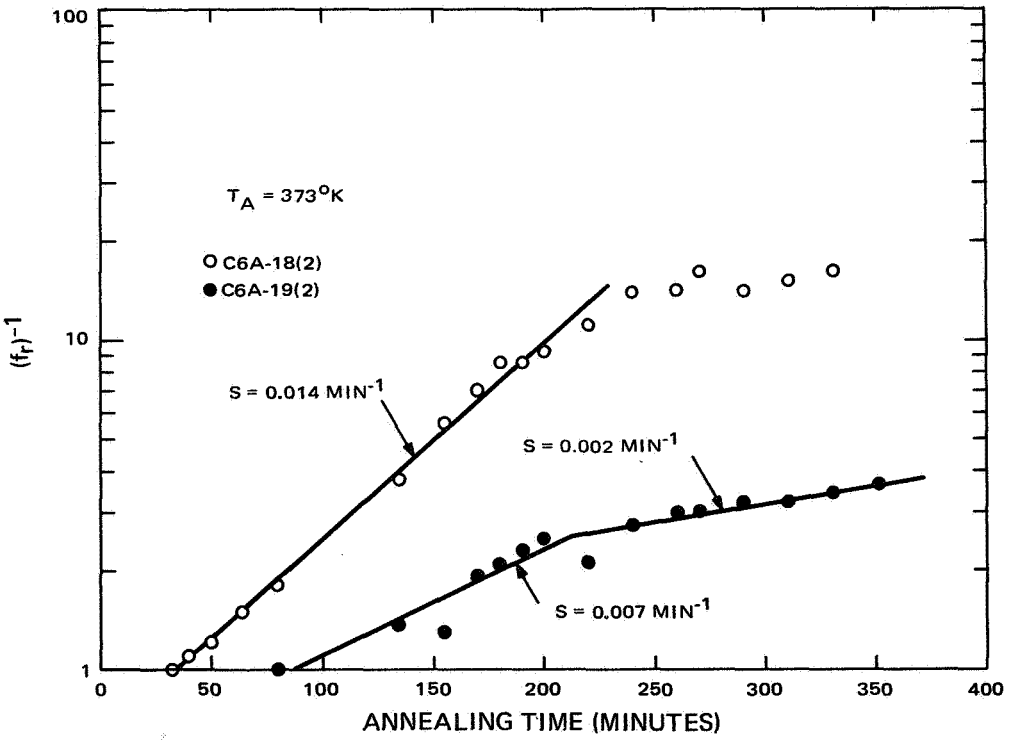

Figure 11. Reciprocal Fraction of Damage Remaining vs Annealing Time at 373°K-Cells C6A-18(2) and C6A-19(2)

Figure 11 gives plots of $(f_r)^{-1}$ vs annealing time for the two cells. This plot is derived from the data of Figure 7: $(f_r)^{-1}$ is given by

$$(f_r)^{-1} = \left(\frac{1}{\tau_{oo}} - \frac{1}{\tau_{oi}}\right) \Big/ \left(\frac{1}{\tau_{ot}} - \frac{1}{\tau_{oi}}\right), \qquad (5)$$

where τ_{oi}, τ_{ot} are the minority-carrier lifetimes at 373°K before irradiation, at the start of recovery, and at a time t after the start of recovery, respectively. In Figure 11, τ_{oo} is taken at the time when the lifetime has reached its minimum value (from the reverse anneal) i.e., at the time when the lifetime has reached its minimum value (from the reverse anneal) i.e., at 33 minutes and 80 minutes for C6A-18(2) and C6A-19(2), respectively. Physically, $[f_r(t)]^{-1}$ is the ratio of the density of unannealed centers at the start of the anneal to that at a time t after the start of annealing. The curve for cell C6A-18(2) is seen to fit a straight line on the semilog plot, with slope $S = 0.014\ \text{min}^{-1}$ fairly well up to $f_r^{-1} \approx 2.5$ and is, subsequently, a good fit to $S \simeq 0.002\ \text{min}^{-1}$. These curves are remarkably similar to annealing curves reported previously (Ref. 1) for FZ cells in which lithium diffusion was clearly responsible for cell recovery. An equation which fits these curves is the equation for first order kinetics (Ref. 1)

$$f_r^{-1} = e^{St}, \quad S = 4\pi N_L D_L r_o \qquad (6)$$

where

N_L is the lithium density,

D_L is the lithium diffusion constant, and

r_o is the capture radius for lithium by the defect.

This would apply to a physical situation where "free" lithium ions diffuse to and are captured by an acceptor-like defect thus neutralizing the defect. Thus, it appears that lithium diffusion is responsible for the annealing. However, this can not be determined with certainty until further experiments, including some with Sb-doped cells without lithium, are performed.

These first results do indicate the possibility that the presence of antimony inhibits lithium diffusion. This possibility will also be investigated in future experiments. Such an inhibiting affect could have major consequences to lithium cell development since a lithium diffusion inhibiting agent with controllable density would then be available.

D. DIODE CHARACTERISTICS AND SURFACE EFFECTS

Cell diode and C-V characteristics of the two cells tested were found to be similar before and after the cells were cut. However, after soldering the cells to the cold finger, some dramatic changes did occur in one of the cells, C6A-19(2). Forward diode characteristics of this cell after cold-finger mounting (and careful cleaning) are shown for various temperatures in Figure 12. The low temperature curves in particular show unusually high empirical A factors ranging up to ≈ 27 in the case of the 83°K curve in the vicinity of 1 mA. Such high A factors are possible only if channels are present (Ref. 15) where the p/n junction is exposed, i.e., at the edges of the cell. Subsequent diode measurements showed significant spontaneous changes in diode characteristic. No further attempts were made to investigate these very complex effects occuring at the cell surfaces although diode measurements were made periodically during the experiment. The data of Figure 12 together with previous data on cell instability due to irregularities in cell diode characteristic (Ref. 1, 3) does, however, suggest the advisability of investigating the possibility of lithium-surface interactions.

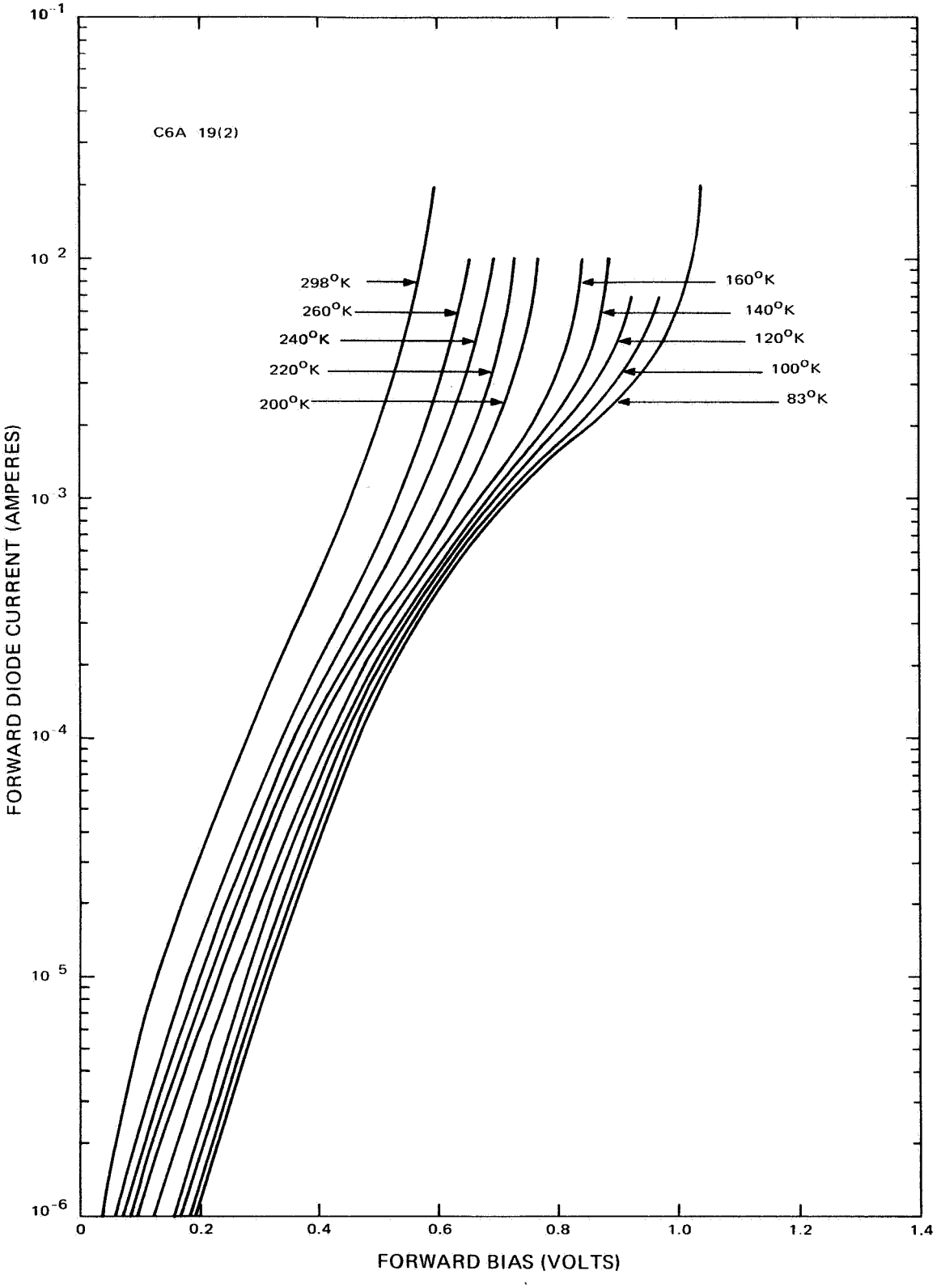

Figure 12. Forward Diode Characteristics of Cell C6A-19(2) After Mounting on Cold Finger

SECTION IV

HALL AND RESISTIVITY MEASUREMENTS

A. INTRODUCTION

The objectives of the Hall and resistivity measurements on bulk-silicon samples diffused with lithium are (1) to determine the dependence of carrier-removal on lithium concentration, oxygen concentration, and electron fluences at low and high bombardment temperatures, and (2) to determine the dependence of annealing at room temperature on the same parameters as for carrier-removal. To achieve these objectives, ingots of high resistivity FZ refined silicon, Monex, and QC grown silicon were procured and are presently being fabricated into Hall bars. Measurements on Hall samples fabricated from silicon procured during the last contract period (Ref. 1) were irradiated and measured. These results will be presented in this report. Some of the properties of samples used to obtain the data in this report are listed in Table V. The lithium density determined from the carrier density measured at room temperature, before and after all bombardments were complete, is listed in columns two and three. Similarly, the Hall mobility of the samples measured at T_M = 79°K to 81°K, before and after bombardment are listed in columns four and five. A complete description of the methods and techniques of these measurements can be found in Reference 1.

TABLE V. FLOAT-ZONE REFINED SILICON ($\rho_o \approx$ 1500 ohm-cm)

Sample	$\Phi = 0$ (Li/cm^3)	$\Phi = \Phi T$ (Li/cm^3)	$\Phi = 0$ $T_M \approx 79°K$ μ (cm^2/sec-volt)	$\Phi = \Phi_T$ $T_M \approx 79°K$ μ (cm^2/sec-volt)
H4-2	3.2×10^{15}		7.9×10^3	2.6×10^3
H4-5	7.2×10^{15}	3.9×10^{15}	7.5×10^3	3.1×10^3
H5-5	1.3×10^{16}	4.3×10^{15}	7.5×10^3	1.8×10^3
H8-1	2×10^{16}	8.4×10^{15}	5.7×10^3	4.5×10^3

B. TEMPERATURE DEPENDENCE OF CARRIER-REMOVAL RATE

Sample H4-2 fabricated from 1500 ohm-cm float-zone refined silicon and diffused with lithium to a concentration of 3.2×10^{15}Li/cm^3 was irradiated at several bombardment temperatures, and then the rate of carrier-removal was determined after each bombardment. These results are shown in Figure 13 together

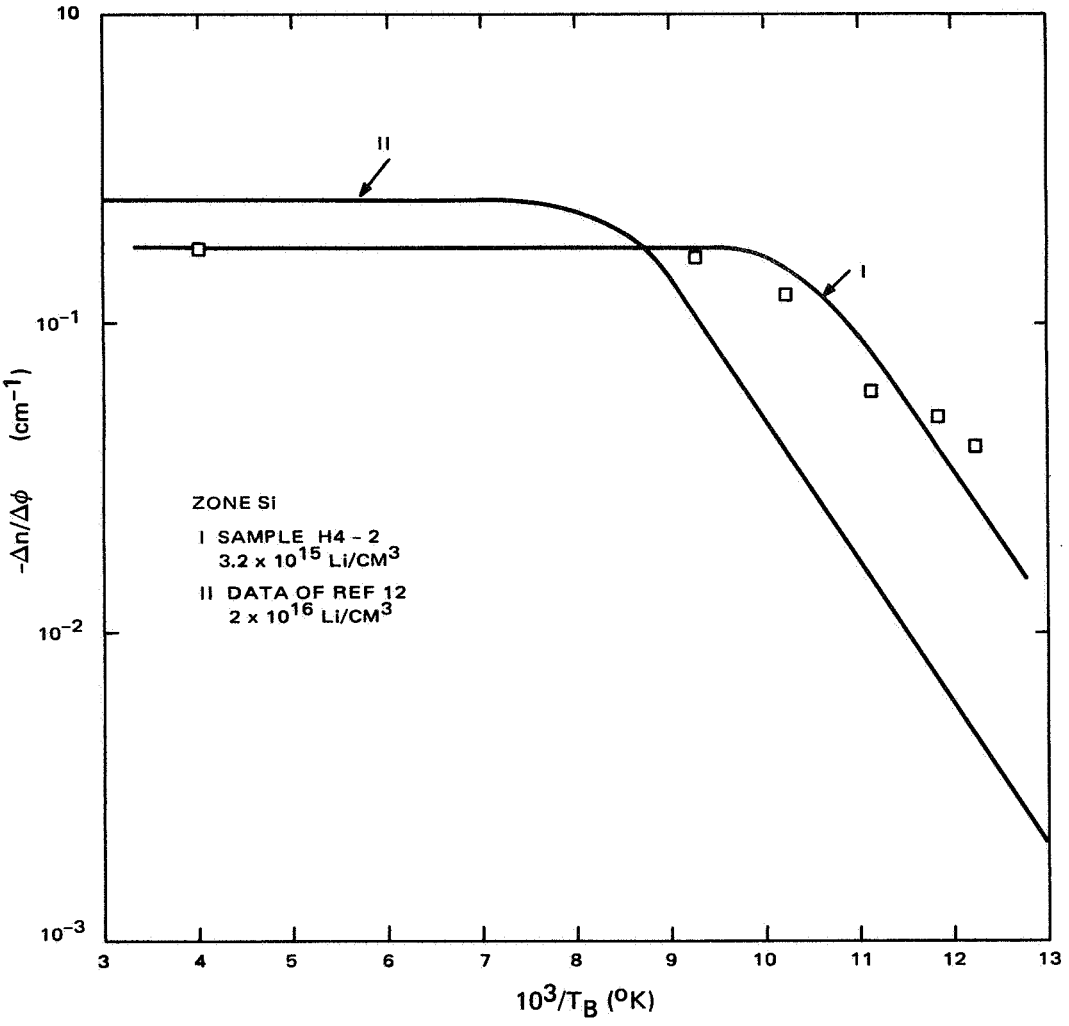

Figure 13. Carrier-Removal Rates vs Reciprocal Bombardment Temperature for Float-Zone (FZ) Silicon. Measurements at 79° to 81°K After Annealing to 200°K. Results of Brucker (Ref. 3) for 0.3 ohm-cm Lithium-Doped FZ Silicon Shown for Comparison.

with the results of Figure I-3, page B-8 of Reference 1. This data of Reference 1 was obtained on four samples of the same lithium concentration, and thus can be accepted with some degree of confidence. Curve I was obtained with only one sample diffused to a lithium concentration approximately an order of magnitude less than the samples used in obtaining Curve II. There are two important points to note, (1) the shift of Curve I along the temperature axis to lower temperatures relative to Curve II, and (2) the lower carrier-removal rate of the higher-resistivity sample (H4-2) at the higher bombardment temperatures. This shift of Curve I was expected since the interstitial-vacancy-close pair model of Reference 16 predicts this dependence of carrier-removal on resistivity. The results of last year's work (Ref. 12) with samples containing 2×10^{16}Li/cm^3 ($\rho = 0.3$ ohm-cm) showed a similar shift to higher temperatures of the carrier-removal curve versus inverse bombardment temperature when compared to the data obtained on 10 ohm-cm phosphorus-doped samples (Ref. 9).

The lower $\Delta n/\Delta\Phi$ value at high bombardment temperatures (e.g., ≈ 0.18 cm^{-1}) in Figure 13 was expected from the work of Reference 17, which indicated that the carrier-removal rate measured on high-resistivity samples bombarded at 270°K is lower than the rates measured on low-resistivity samples. However, no physical explanation has yet been put forward for this behavior and at least three to four samples of the same resistivity should be measured before any definite conclusions can be made concerning this effect. In contrast to this situation, evidence for shift of the carrier-removal curve along the temperature axis, controlled by resistivity, is already firm.

C. FLUENCE DEPENDENCE OF CARRIER-REMOVAL RATE

Measurements of the fluence dependence of carrier-removal in irradiated silicon have been made and reported on in the literature (Ref. 17-19). Samples doped with conventional impurities (e.g., phosphorus, antimony, and arsenic) and with lithium have been investigated by other workers. It is one of the objectives of this work to determine the influence of the degree of damage on the annealing properties at room temperature of lithium-doped silicon. It has been shown (Ref. 18-19) that, for a fixed temperature of bombardment and measurement, the carrier-removal rate decreases exponentially with fluence when the removal rate and damage level is high. However, if the removal rate is low, then it has been shown (Ref. 9, 12, and 17) that carriers are removed linearly with fluence, and the carrier-removal rate is constant over a limited range of fluences. However, the situation is more complex when the bombardment temperature and/or measuring temperature are varied. This is illustrated in Figure 14 where the curves of carrier density, n versus fluence, Φ measured at two temperatures on sample H5-5 are shown. This sample had been bombarded at lower temperatures prior to the bombardment at $T_B = 250$°K. However, the major part of the damage occurred during the bombardment at the higher temperature. The sample was measured at a temperature of 250°K, and at 79°K. The latter level has been used throughout this work as a reference temperature.

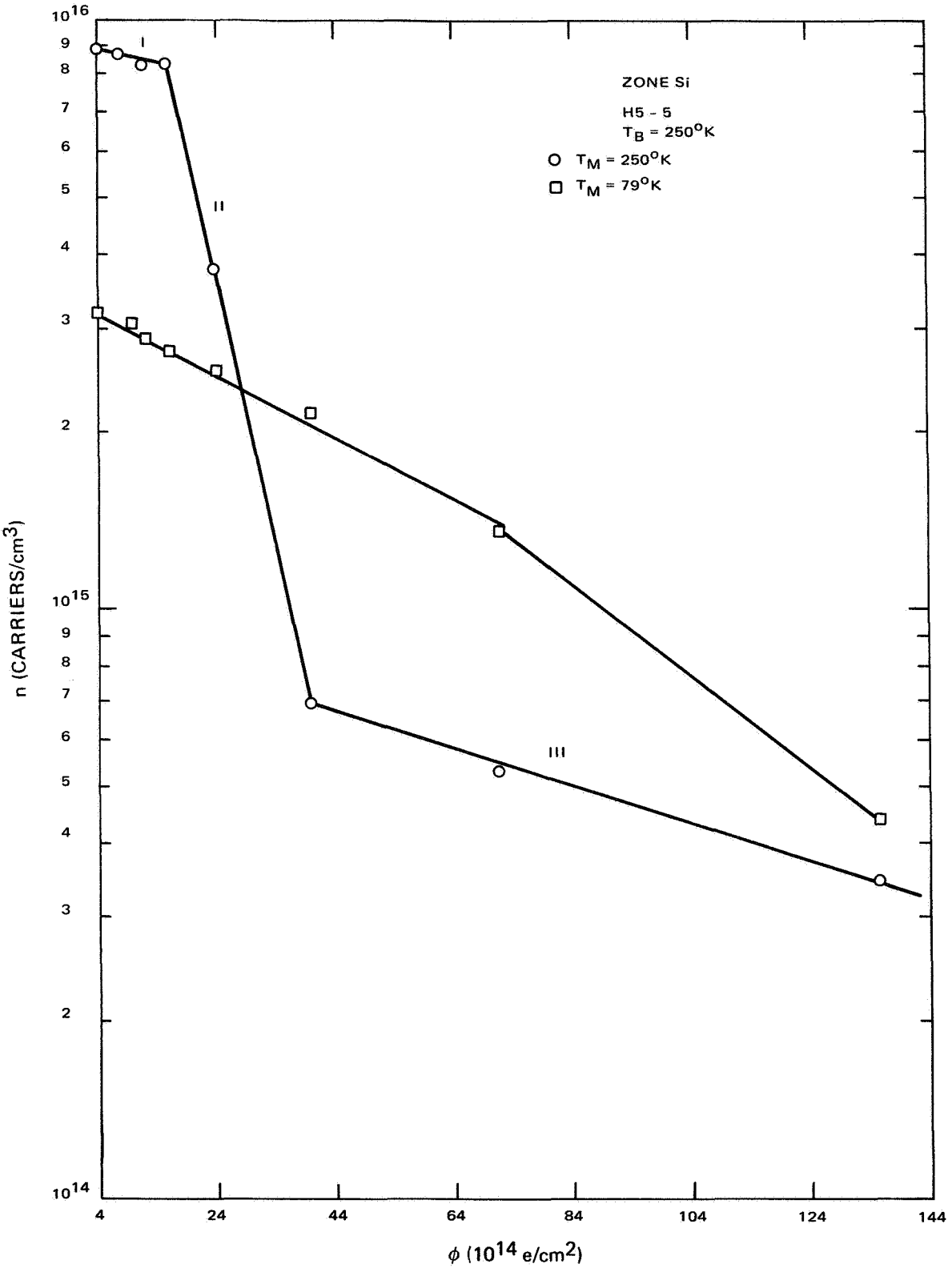

Figure 14. Carrier Density versus Fluence for FZ Silicon Sample (H5-5) Bombarded at 250°K and Measured at 79° and 250°K

The results in Figure 14 demonstrate that carrier-removal rates measured at high temperature can be lower or higher than those measured at low temperature. There is agreement in carrier-removal rates determined in region I of the curve measured at $T_M = 250°K$, where the fluence and carrier losses are small. In region II, the carrier-removal rate $\eta\,(T_M = 250°K) \approx 12\eta\,(T_M = 79°K)$, and in region III $\eta\,(T_M = 250°K) \approx 0.2\eta\,(T_M = 79°K)$. Obviously the curves for $T_M = 79°K$ can be fitted with an exponential dependence on Φ and a single constant (for example, $n = n_0 e^{-\beta\Phi}$). Three different constants are required to fit the curve obtained for $T_M = 250°K$ in the three regions labeled I, II, and III in Figure 14. These results point out the complexity of the physical situation and the necessity for care in comparing the results of different experiments.

This sample (H5-5) was annealed at room temperature for some time until the carrier density had increased considerably from the value measured immediately after completion of the bombardment. Following this recovery of the carrier density, the sample was bombarded at room temperature, and measured at both room temperature and 79°K. These results are shown in Figure 15. Note that $\eta\,(T_M = 297°K)$ is slightly greater than $\eta\,(T_M = 70°K)$. It appears that the irradiation history and/or long room temperature bombardments which are accompanied by annealing can modify the measured carrier-removal rates.

D. ANNEALING AT ROOM TEMPERATURE

1. Carrier Density Changes

One of the important properties of irradiated lithium-doped silicon is the annealing at room temperature (297°K) of the damage, and recovery of electrical parameters to their pre-irradiation values. Results of annealing studies obtained on three samples are shown in Figure 16 where the unannealed fraction f_n of carrier density versus annealing time at a temperature of 297°K is given. Sample H5-4 was bombarded at 200°K, then allowed to anneal. The other two samples were irradiated at several temperatures and then annealed. Sample H5-5 was bombarded and annealed in several cycles. First order annealing kinetics describe the behavior for approximately the first hour of annealing time. After this period of time, a second stage of recovery takes place which is unstable, and the carrier density decreases to some equilibrium level. Both samples H4-5 and H8-1 showed this effect. Sample H5-5 could have behaved similarly, however measurements were not made during the annealing time when this effect seemed to occur.

The behavior of the lithium concentration during the annealing cycle can be inferred from the behavior of the carrier density measured at a temperature of 297°K. These results are shown in Figure 17 where the unannealed carrier density f_n versus annealing time is shown. All three samples exhibited a recovery of the

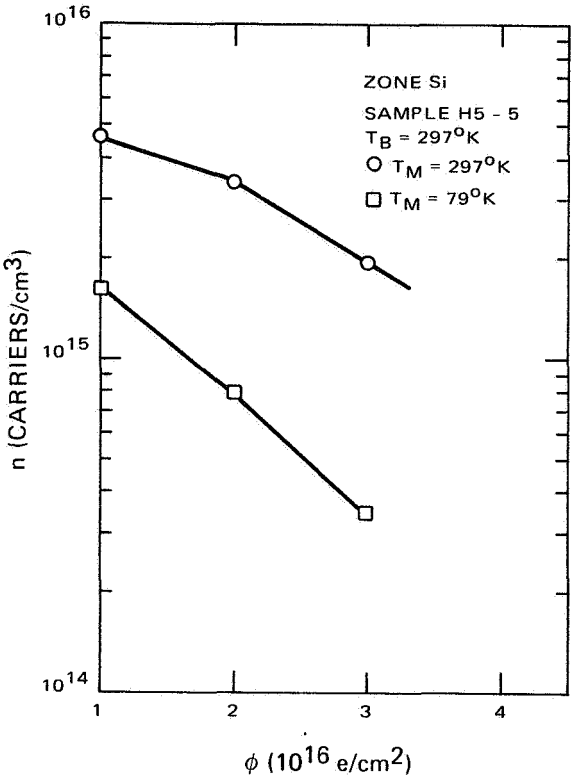

Figure 15. Carrier Density versus Fluence for FZ Silicon Sample (H5-5) Bombarded at 297°K Following an Annealing Cycle at Room Temperature. Measurement Made at 79° and 197°K are Shown

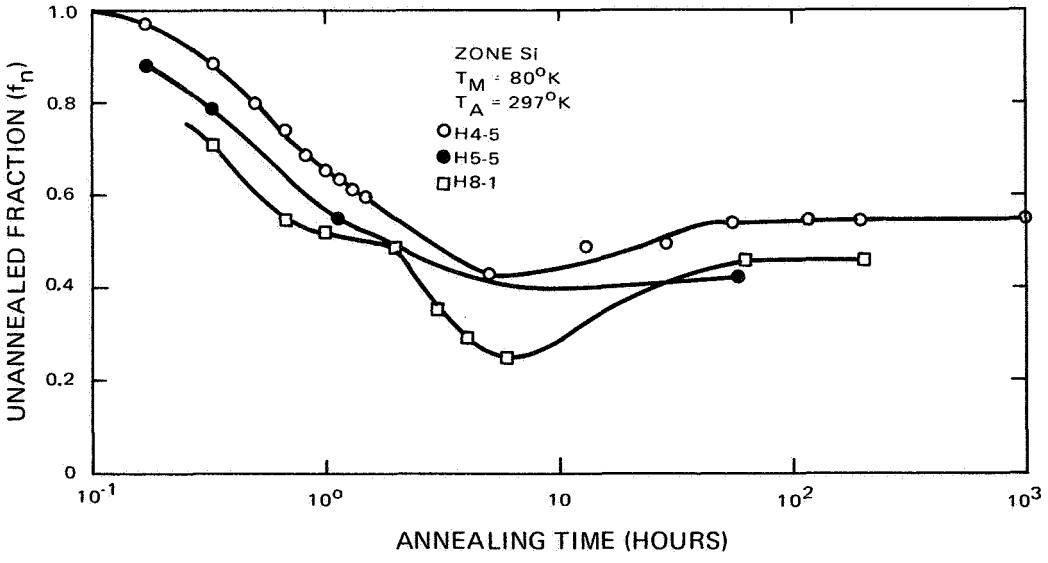

Figure 16. Unannealed Fraction of Carrier Density versus Annealing Time for Three Samples of FZ Silicon Annealed at a Temperature of 297°K and Measured at 79° to 80°K

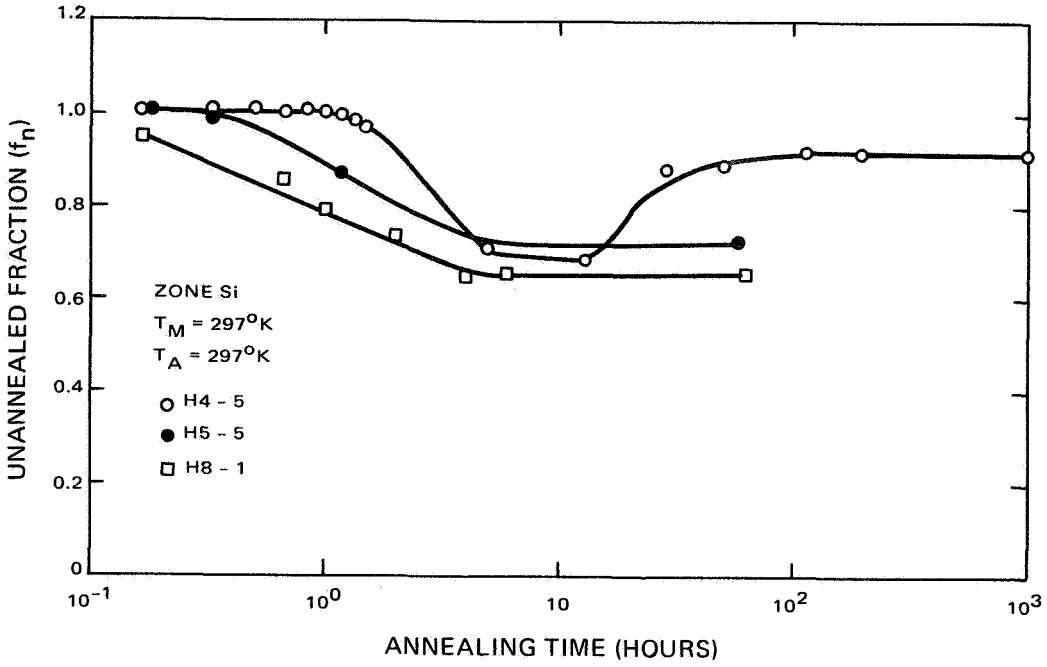

Figure 17. Unannealed Fraction of Carrier Density versus Annealing Time for Three Samples of FZ Silicon Annealed and Measured at a Temperature of 297°K

lithium concentration during the annealing cycle. This recovery has been explained in Reference 12 as evidence for the instability of the LiV complex, and therefore its subsequent dissociation which returns free lithium to the crystal. Sample H4-5 showed that the formation of the LiV defect or some other defect involving lithium can also take place after dissociation occurred. It should be noted that the fastest recovery was shown by the sample with the highest lithium concentration. Sample H5-5 had a slightly lower lithium concentration than H8-1, but higher than sample H4-5. These results are in agreement with the results obtained on solar cells (Ref. 1 and 20).

2. Mobility Changes

The Hall and resistivity measurements made during the annealing cycles enable us to determine the behavior of the mobility. These results are shown in Figure 18 where the unannealed fraction of the reciprocal of the mobility versus annealing time is shown. The recovery-time dependence of the mobility on lithium concentration is in agreement with the data of Figures 16 and 17. Recovery of the mobility demonstrates that electrical neutralization of charged-scattering defects occurs during the room temperature annealing cycles. The author in Reference 12 described the neutralization as due to a complexing of lithium with

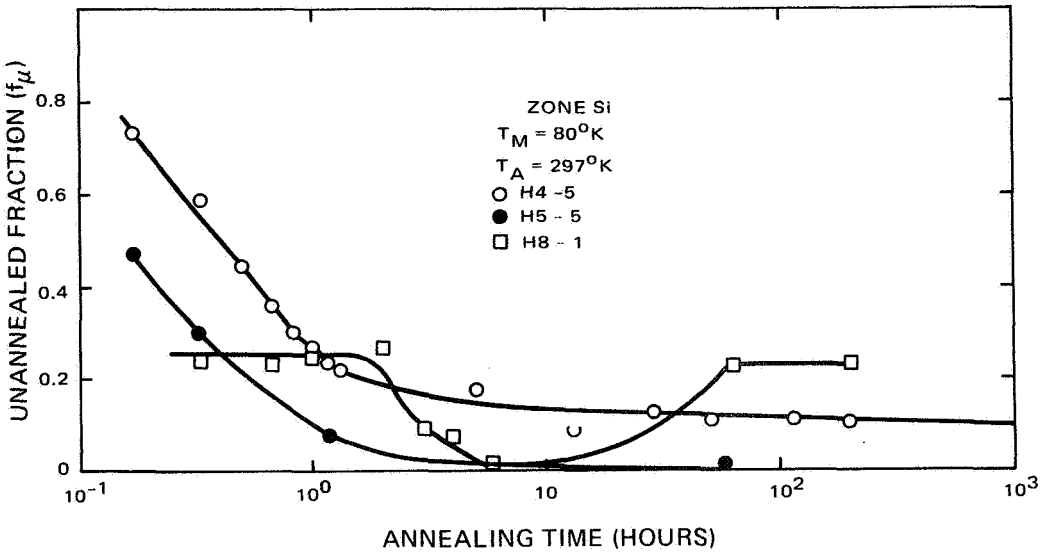

Figure 18. Unannealed Fraction of Reciprocal Mobility versus Annealing Time for the Sample of FZ Silicon Annealed at a Temperature of 297°K and Measured at 79° to 80°K

a LiV^- acceptor so as to neutralize the negative charge. The unstable behavior of the mobility after an annealing time of approximately one hour was shown by sample H8-1, but not by the other two samples within the accuracy of the measurements. It appears that the tendency towards instability in the mobility or carrier-density recovery was greater in the sample of lower resistivity. The similarity of these annealing curves to the data obtained on solar cells (Ref. 1 and 20) can be seen by replotting the data of Figure 18 in Figure 19, where the log of the reciprocal-unannealed fraction versus time is given. These curves are very similar to the solar cell curve of References 1 and 20, and also this report.

E. EFFECT OF IRRADIATION HISTORY ON ANNEALING

The investigation of the effects of irradiation history by repeated annealing cycles is only in a very preliminary stage, but it is now apparent that the conditions of the experiment must be carefully controlled for meaningful comparisons to be made. However, three cycles of annealing data obtained on sample H4-5 are shown in Figures 20 and 21 where the unannealed fraction of carrier density and the unannealed fraction of reciprocal mobility versus annealing time are plotted. The interesting point in Figures 8 and 9 is the apparent increase of

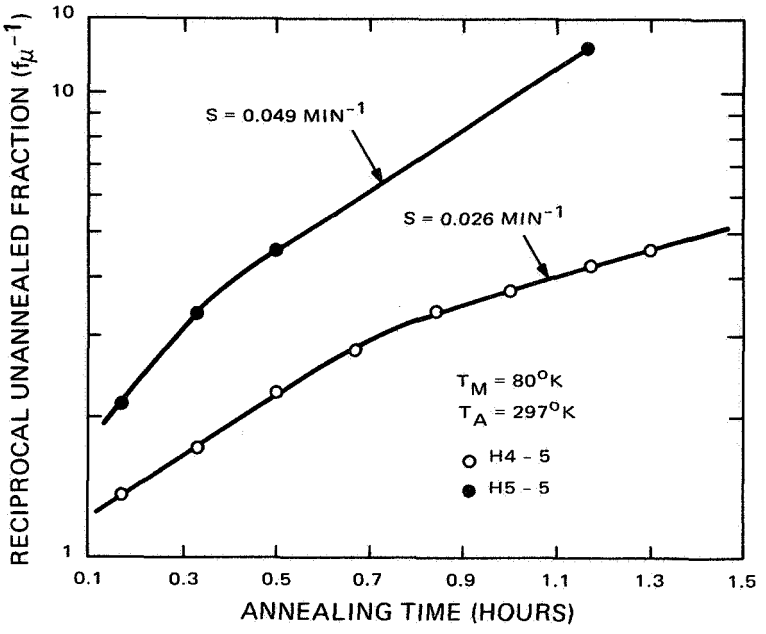

Figure 19. Reciprocal of Unannealed Fraction of Reciprocal Mobility versus Annealing Time for Two Samples of FZ Silicon Annealed at a Temperature of 297°K and Measured at 79° to 80°K

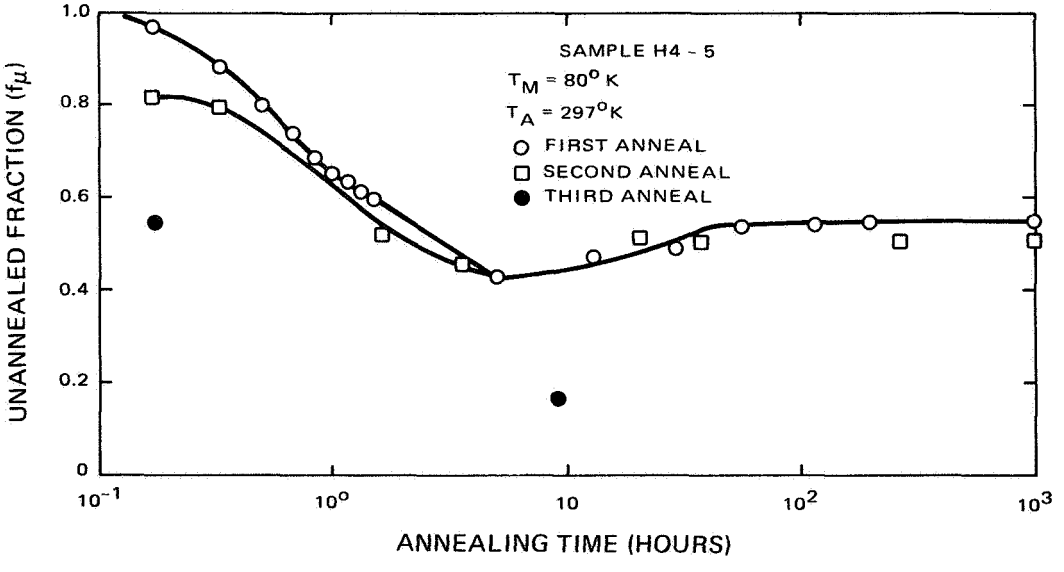

Figure 20. Unannealed Fraction of Carrier Density versus Annealing Time for One Sample of FZ Silicon bombarded and annealed at 297°K for Three Successive Cycles and Measured at 80°K

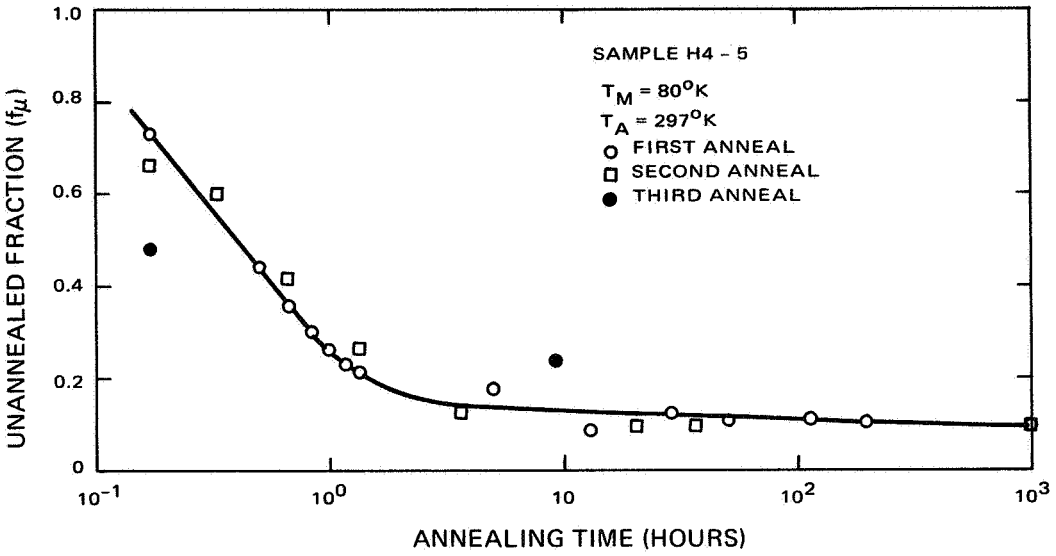

Figure 21. Unannealed Fraction of Reciprocal Mobility versus Annealing Time for One Sample of FZ Silicon Bombarded and Annealed at 297° K for Three Successive Cycles and Measured at 80°K

recovery speed with repeated annealing cycles. This is probably due to the greater degree of damage produced in the sample prior to the first annealing cycle compared to the succeeding two cycles. The lithium concentration at the start of any of the annealing cycles was approximately the same for all three cycles but the pre-irradiation concentration measured prior to the first bombardment was 2-1/2 times greater than the concentration measured prior to the second and third run. These results agree with solar cell behavior which showed the same dependence of recovery time on fluence.

F. DISCUSSION OF RESULTS AND SUMMARY

1. It is still too soon in our investigation to be any definite conclusions or explanations of the results presented in this report. Only possible trends can be pointed out until the statistics of our measurements are improved.

The temperature dependence of carrier-removal rate on resistivity (lithium concentration) appears to agree with the predictions of the interstitial-vacancy close-pair model (Ref. 16) It appears that the carrier-removal rate at high temperatures increases with lithium concentration. This is not physically explainable at the present time but this trend is in agreement with the experimental observations of Stein and Gereth (Ref. 17).

2. The results of the fluence dependence studies show that the level of damage and temperature of measurement is important, and both parameters must be considered in any cross-comparison of carrier-removal rates obtained from different experimental set-ups. It is interesting to note that the carrier-removal measurements made at low temperature (≈79°K, see Figure 14 were less dependent on fluence than those made at high temperature. This behavior would be consistent with a Fermi-level effect if shallow defect levels were produced by the bombardments. However, the experimental results indicate that in irradiated lithium-doped float-zone-refined silicon (Ref. 12), the radiation-induced defect levels are deep in the forbidden gap, and thus the position of the Fermi level should not have any effect on the measurement of carrier density due to the presence of shallow acceptors. Nevertheless; the Fermi level will determine whether the lithium donor level is ionized or neutral, and, hence, the Fermi-level can influence the measurements in this way.

3. The preliminary annealing studies were particularly gratifying since it appears that a qualitative correlation of the annealing behavior of irradiated silicon with the annealing behavior of solar cells was observed. Agreement was observed in the following annealing properties, (a) type of kinetics (first order), and (b) dependence of recovery time on lithium concentration and damage level. Additional evidence of the dissociation and complexing of lithium with defects during room temperature annealing was obtained. This is consistent with our previous work (Ref. 12). There appears to be a tendency for an instability in the recovery of carrier density and mobility to occur in the more heavily-doped samples, but this will require further investigation before any definite conclusions can be stated.

SECTION V

CONCLUSIONS AND FUTURE WORK

A. SOLAR CELL STABILITY

The general conclusions drawn from last year's work (Ref. 1) on lithium cell stability have been further confirmed in recent work, namely:

(1) high values of lithium density ($\gtrsim 3 \times 10^{15} cm^{-3}$) and density gradient ($> 10^{19} cm^{-4}$) in oxygen-lean silicon give cells which have a significant degree of instability. The instability can show up in short-circuit current, open-circuit voltage or curve power factor or in combinations of these. However, one lot of QC cells with moderately high density gradient ($\sim 2 \times 10^{19} cm^{-4}$, Hl-cells) have shown good stability. Another lot with high gradient ($\sim 5 \times 10^{19} cm^{-4}$, T7-cells) show significant re-degradation, ~3 percent in power and current.

(2) QC cells anneal at rates about 2 orders of magnitude slower than FZ or Lopex cells of equal density. QC cells of Lot T2 which annealed very rapidly are a notable exception.

(3) A wide range of lithium cells achieves recovered outputs after irradiation significantly above those obtained for 10 ohm-cm n/p control cells.

(4) Cells with low lithium density gradient (i.e., below about $3 \times 10^{18} cm^{-4}$) have satisfactory stability. However these cells develop series resistance after high fluences, presumably due to extensive carrier removal.

(5) In general, cells with moderate lithium density gradients ($< 10^{19} cm^{-4}$) near the junction have satisfactory stability. An exception to this has been found, however, in the latest measurements on C4 cells where batch III and V cells suffer ≈2 percent short-circuit current degradation which is independent of electron fluence.

Additional new findings are:

(1) Study of two batches of cells (T3 and T5) indicate that no changes were introduced in cell recovery behavior by a process change, namely, changing from lithium diffusion into individual cell blanks (i.e., after cutting) to lithium diffusion into whole wafers (i.e., before cutting). This suggests that non-uniform lithium concentrations at the cell edge does not affect recovery behavior.

(2) Group T8 cells, apparently fabricated and processed like T7 cells, actually behave quite differently.

(3) Antimony-doped QC cells (C2) have displayed ≈3 percent recovery in short-circuit current 280 days after irradiation to $1 \times 10^{14} e/cm^2$.

B. LOW TEMPERATURE EXPERIMENTS

Diffusion-length vs temperature measurements on two QC-grown, antimony-doped lithium cells irradiated to a fluence of $3 \times 10^{15} e/cm^2$ show a defect level at $\approx E_C - 0.16$ V which is probably the A-center. This level appears to be slightly modified during annealing at 373°K in that the defect level fits $\approx E_C - 0.15$ V after annealing. Significant minority-carrier lifetime recovery occurred in both cells during the 6-hour anneal at 373°K, however, the cell more heavily doped with antimony recovered less in the same time than the more lightly doped cell. The recovery kinetics were approximately first order. It is tentatively concluded that lithium diffusion was responsible for this recovery; further experiments will be made to test this conclusion and the possible special role of antimony in the behavior of these cells.

C. HALL MEASUREMENTS

It was stated before that no definite conclusions can be stated because of the poor statistics of the experiments at this preliminary stage in the investigations. However, the trend of the results concerning the dependence of carrier-removal rate, and annealing on resistivity appears to be as expected. Thus, (1) the temperature dependence of the carrier-removal rate appears to shift to lower temperatures with lower lithium concentration, (2) the removal rate measured at high bombardment temperature (T_B = 140°K to 297°K) appears to decrease with decreasing lithium concentration, and (3) recovery-time constants are increased with decrease of the lithium density. It will be the immediate objective of future investigations to confirm these trends.

D. FUTURE PLANS

The stability tests will be continued on the cells. More irradiations of solar cells will be conducted on the cold finger apparatus. Hall and resistivity measurements will also be continued. Further tests will be made to check the possible special role of antimony in the slow recovery of some antimony-doped QC solar cells. The eventual goal of this effort is to understand the damage and recovery mechanisms so that an optimum set of design rules can be specified.

REFERENCES

1. G.J. Brucker, T.J. Faith and A.G. Holmes-Siedle, Final Report, JPL Contract No. 952249, prepared by RCA and issued April 21, 1969.

2. M. Wolf and H. Rauschenbach, Adv. Energy Conversion 3, 455 (1963).

3. T.J. Faith, G.J. Brucker, A.G. Holmes-Siedle and J. Wysocki, Conf. Record of the Seventh Photovoltaic Spec. Conf., IEEE Catalog No. 68C63ED, 131 (1968).

4. W. Rosenzweig, Bell Sys. Tech. Journ. 41, 1573 (1962).

5. F.J. Morin and J.P. Maita, Phys. Rev. 96, 28 (1954).

6. R.N. Hall, Phys. Rev. 83, 228 (1951) and 87, 387 (1952).

7. W. Shockley and W.T. Reed, Jr., Phys. Rev. 87, 835 (1952).

8. J.A. Baicker, Phys. Rev. 129, 1174 (1963).

9. H.J. Stein and F.L. Vook, Phys. Rev. 163, 790 (1967).

10. G.K. Wertheim, Phys. Rev. 115, 568 (1959).

11. R.L. Novak, Ph.D. Thesis, University of Pennsylvania (1964).

12. G.J. Brucker, Phys. Rev., 183, 712, (1969).

13. H.M. DeAngelis, C.P. Carnes, P.J. Drevinsky and R.E. Penczer, Bull. Amer. Phys. Soc. 13, Series II, 380 (1968).

14. M. Hirata, M. Hirata, and H. Saito, Japan. J. Appl. Phys. Vol 5, pp 252, 1966.

15. C.T. Sah, IRE Trans. Electron Devices ED-9, 94 (1962).

16. F.L. Vook and H.J. Stein, "Production of Defects in N-Type Silicon," Proceedings of the Santa Fe Conference on Radiation Effects in Semiconductors, Plenum-Press, N.Y. pp 99-114, Oct. 1967.

17. H.J. Stein and R. Gereth, J. Appl. Phys. Vol. 39, pp 2890, 1968.

18. R.G. Downing, J.R. Carter, R.E. Scott, and W.K. Van Atta, TRW Final Report, Contract No. 952251, May 27, 1969.

19. B. Goldstein, RCA Final Report, Contract No. F19628-68- C-0133, Nov. 1, 1967 to July 31, 1968.

20. J.J. Wysocki, G.J. Brucker and A.G. Holmes-Siedle, Final Report, NASA Contract No. NAS5-10239, prepared by RCA and issued June 1967.